

# Genomic and drug target evaluation of 90 cardiovascular proteins in 30,931 individuals

Lasse Folkersen<sup>1,2\*</sup>, Stefan Gustafsson<sup>3\*</sup>, Qin Wang<sup>4,5\*</sup>, Daniel Hvidberg Hansen<sup>6</sup>, Åsa K Hedman<sup>1,7</sup>, Andrew Schork<sup>8,9</sup>, Karen Page<sup>10</sup>, Daria V Zhernakova<sup>11</sup>, Yang Wu<sup>12</sup>, James Peters<sup>13</sup>, Niclas Eriksson<sup>14</sup>, Sarah E Bergen<sup>15</sup>, Thibaud Boutin<sup>16</sup>, Andrew D Bretherick<sup>16</sup>, Stefan Enroth<sup>17</sup>, Anette Kalnapenkis<sup>18</sup>, Jesper R Gådin<sup>1</sup>, Bianca Suur<sup>19</sup>, Yan Chen<sup>1</sup>, Ljubica Matic<sup>19</sup>, Jeremy D Gale<sup>20</sup>, Julie Lee<sup>10</sup>, Weidong Zhang<sup>21</sup>, Amira Quazi<sup>10</sup>, Mika Ala-Korpela<sup>4,5,22</sup>, Seung Hoan Choi<sup>23</sup>, Annique Claringbould<sup>11</sup>, John Danesh<sup>13</sup>, George Davey-Smith<sup>24</sup>, Federico de Masi<sup>6</sup>, Sölve Elmståhl<sup>25</sup>, Gunnar Engström<sup>25</sup>, Eric Fauman<sup>26</sup>, Celine Fernandez<sup>25</sup>, Lude Franke<sup>11</sup>, Paul Franks<sup>27</sup>, Vilmantas Giedraitis<sup>28</sup>, Chris Haley<sup>16</sup>, Anders Hamsten<sup>1</sup>, Andres Ingason<sup>8</sup>, Åsa Johansson<sup>17</sup>, Peter K Joshi<sup>29</sup>, Lars Lind<sup>30</sup>, Cecilia M. Lindgren<sup>31,32,23</sup>, Steven Lubitz<sup>33,23</sup>, Tom Palmer<sup>34</sup>, Erin Macdonald-Dunlop<sup>29</sup>, Martin Magnusson<sup>35,36</sup>, Olle Melander<sup>25</sup>, Karl Michaelsson<sup>37</sup>, Andrew P. Morris<sup>38,39,32</sup>, Reedik Mägi<sup>18</sup>, Michael W Nagle<sup>26</sup>, Peter M Nilsson<sup>25</sup>, Jan Nilsson<sup>25</sup>, Marju Orho-Melander<sup>40</sup>, Ozren Polasek<sup>41</sup>, Bram Prins<sup>13</sup>, Erik Pålsson<sup>42</sup>, Ting Qi<sup>12</sup>, Marketa Sjögren<sup>25</sup>, Johan Sundström<sup>43</sup>, Praveen Surendran<sup>13</sup>, Urmo Vösa<sup>18</sup>, Thomas Werge<sup>8</sup>, Rasmus Wernersson<sup>6</sup>, Harm-Jan Westra<sup>11</sup>, Jian Yang<sup>12,44</sup>, Alexandra Zhernakova<sup>11</sup>, Johan Ärnlöv<sup>45</sup>, Jingyuan Fu<sup>11,46</sup>, Gustav Smith<sup>47</sup>, Tonu Esko<sup>18,23</sup>, Caroline Hayward<sup>16</sup>, Ulf Gyllenstein<sup>17</sup>, Mikael Landen<sup>42</sup>, Agneta Siegbahn<sup>48</sup>, Jim F Wilson<sup>29,16</sup>, Lars Wallentin<sup>49</sup>, Adam S Butterworth<sup>13</sup>, SCALLOP consortium, Michael V Holmes<sup>50\*</sup>, Erik Ingelsson<sup>51\*</sup>, Anders Mälarstig<sup>1,52\*</sup>

\* these authors contributed equally

- 1 Department of Medicine, Solna, Karolinska Institute, Sweden
- 2 Danish National Genome Center, Copenhagen, Denmark
- 3 Department of Medical Sciences, Molecular Epidemiology and Science for Life Laboratory, Uppsala University, Uppsala, Sweden
- 4 Systems Epidemiology, Baker Heart and Diabetes Institute, Melbourne, VIC, Australia
- 5 Computational Medicine, Faculty of Medicine, University of Oulu and Biocenter Oulu, Oulu, Finland
- 6 Intomics, Lottenborgvej 26, 2800 Lyngby (Copenhagen), Denmark
- 7 Pfizer Worldwide Research & Development, Cambridge, MA, USA
- 8 Institute of Biological Psychiatry, Mental Health Center Sct. Hans, Mental Health Services Capital Region, Roskilde, Denmark
- 9 Neurogenomics Division, The Translational Genomics Research Institute (TGEN), Phoenix, AZ, USA
- 10 Early Clinical Development, Pfizer Worldwide Research & Development, Cambridge, MA, USA
- 11 University of Groningen, University Medical Center Groningen, Department of Genetics, Groningen, the Netherlands
- 12 Institute for Molecular Bioscience, The University of Queensland, Brisbane, Queensland, Australia
- 13 BHF Cardiovascular Epidemiology Unit, Department of Public Health and Primary Care, University of Cambridge, United Kingdom
- 14 Department of Medical Sciences, Uppsala Clinical Research Center, Uppsala University, Uppsala, Sweden
- 15 Department of Medical Epidemiology and Biostatistics, Karolinska Institutet, Stockholm, Sweden
- 16 MRC Human Genetics Unit, Institute of Genetics and Molecular Medicine, University of Edinburgh, Western General Hospital, Crewe Road, Edinburgh, EH4 2XU, Scotland
- 17 Department of Immunology, Genetics, and Pathology, Biomedical Center, Science for Life Laboratory (SciLifeLab) Uppsala, Box 815, Uppsala University, SE-75108 Uppsala, Sweden
- 18 Estonian Genome Center, Institute of Genomics, University of Tartu 51010, Estonia
- 19 Department of Molecular Medicine and Surgery, Solna, Karolinska Institute, Sweden
- 20 Inflammation and Immunology Research Unit, Pfizer Worldwide Research & Development, Cambridge, MA, USA
- 21 Pfizer Global Product Development, Cambridge, MA, USA
- 22 NMR Metabolomics Laboratory, School of Pharmacy, University of Eastern Finland, Kuopio, Finland
- 23 Program in Medical and Population Genetics, Broad Institute, Cambridge, MA, USA
- 24 MRC Integrative Epidemiology Unit, University of Bristol, UK
- 25 Department of Clinical Sciences, Lund University, Skåne University Hospital, Malmö, Sweden
- 26 Internal Medicine Research Unit, Pfizer Worldwide Research & Development, Cambridge, MA, USA
- 27 Lund University Diabetes Center, Department of Clinical Sciences, Malmö, Sweden
- 28 Department of Public Health and Caring Sciences/Geriatrics, Uppsala University, Uppsala, Sweden.
- 29 Centre for Global Health Research, Usher Institute for Population Health Sciences and Informatics, University of Edinburgh, Teviot Place, Edinburgh, EH8 9AG, Scotland
- 30 Department of Medical Sciences, Uppsala University, Uppsala, Sweden.
- 31 Big Data Institute at the Li Ka Shing Centre for Health Information and Discovery, University of Oxford, Oxford, United Kingdom.
- 32 Wellcome Centre for Human Genetics, Nuffield Department of Medicine, University of Oxford, Oxford, United Kingdom.
- 33 Cardiovascular Research Center, Massachusetts General Hospital, United States.
- 34 Department of Mathematics and Statistics, University of Lancaster, Lancaster, UK

60 35 Department of Cardiology, Skåne University Hospital Malmö, Malmö, Sweden  
61 36 Wallenberg Center for Molecular Medicine, Lund University, Lund, Sweden  
62 37 Department of Surgical Sciences, Uppsala University, Uppsala, Sweden  
63 38 Division of Musculoskeletal and Dermatological Sciences, University of Manchester, Manchester, UK  
64 39 Department of Biostatistics, University of Liverpool, Liverpool, UK  
65 40 Department of Clinical Sciences, Clinical Research Center, Lund University, Malmö, Sweden  
66 41 Faculty of Medicine, University of Split, Split, Croatia  
67 42 Department of Psychiatry and Neurochemistry, Institute of Neuroscience and Physiology, the Sahlgrenska Academy at the University of Gothenburg,  
68 Gothenburg, Sweden  
69 43 Department of Medical Sciences, Clinical Epidemiology, Uppsala University, Uppsala, Sweden; and The George Institute for Global Health, University of New  
70 South Wales, Sydney, Australia  
71 44 Institute for Advanced Research, Wenzhou Medical University, Wenzhou, Zhejiang 325027, China  
72 45 Department of Neurobiology, Care Sciences and Society (NVS), Division of Family Medicine and Primary Care, Karolinska Institutet, Sweden  
73 46 University of Groningen, University Medical Center Groningen, Department of Paediatrics, Groningen, the Netherlands  
74 47 Department of Cardiology, Clinical Sciences, Lund University, Skåne University Hospital, Lund, Sweden.  
75 48 Department of Medical Sciences, Clinical Chemistry, Uppsala University, Uppsala, Sweden  
76 49 Department of Medical Sciences, Cardiology and Uppsala Clinical Research Center, Uppsala University, Uppsala, Sweden  
77 50 Clinical Trial Service Unit and Epidemiological Studies Unit (CTSU), Nuffield Department of Population Health, University of Oxford, Oxford, United Kingdom.  
78 51 Department of Medicine, Division of Cardiovascular Medicine, Falk Cardiovascular Research Center, Stanford University School of Medicine, 300 Pasteur  
79 Drive, CV 273, Stanford, CA, 94305, USA.  
80 52 Emerging Science & Innovation, Pfizer Worldwide Research & Development, Cambridge, MA, USA  
81

82 Corresponding author: Anders Mälarstig [anders.malarstig@ki.se](mailto:anders.malarstig@ki.se)

83

84

85

86 **Abstract**

87

88 Circulating proteins are vital in human health and disease and are frequently used as biomarkers for  
89 clinical decision-making or as targets for pharmacological intervention. Here we map and replicate  
90 protein quantitative trait loci (pQTL) for 90 cardiovascular proteins in over 30,000 individuals,  
91 resulting in 451 pQTLs for 85 proteins. For each protein we further perform pathway mapping to  
92 obtain trans-pQTL gene and regulatory designations. We substantiate these regulatory findings with  
93 orthogonal evidence for trans-pQTLs using mouse knock-down experiments (ABCA1, TRIB1) and  
94 clinical trial results (CCR2, CCR5), with consistent regulation. Finally we evaluate known drug targets,  
95 and suggest new target candidates or repositioning opportunities using Mendelian randomization.  
96 This identifies 11 proteins with causal evidence of involvement in human disease that have not  
97 previously been targeted, including (gene symbols) EGF, IL16, PAPP, SPON1, F3, ADM, CASP8,  
98 CHI3L1, CXCL16, GDF15, and MMP12. Taken together these findings demonstrate the utility of large-  
99 scale mapping the genetics of the proteome, and provide a resource for future precision studies of  
100 circulating proteins in human health.

101

102

103

104

105

106

107

108

109

## 110 Main

111 Proteins circulating in blood are derived from multiple organs and cell types, and consist of both  
112 actively secreted and passively leaked proteins. Plasma proteins are frequently used as biomarkers to  
113 diagnose and predict disease and have been of key importance for clinical practice and drug  
114 development for many decades.

115 Circulating proteins are attractive as potential drug targets as they can often be directly perturbed  
116 using conventional small molecules or biologics such as monoclonal antibodies<sup>1</sup>. However, a  
117 prerequisite for successful drug development is efficacy, which is predicated on the drug target  
118 playing a causal role in disease. One approach to clarifying causation is through Mendelian  
119 randomization (MR), which has successfully predicted the outcome of randomized controlled trials  
120 (RCT) for pharmacological targets such as PCSK9, LpPLA2 and NPC1L1, and is increasingly becoming a  
121 standard tool for triaging new drug targets<sup>2</sup>.

122 Recent technological developments of targeted proteomic methods have enabled hundreds to  
123 thousands of circulating proteins to be measured simultaneously in large studies<sup>3-6</sup>. This has paved  
124 the way for studies of genetic regulation of circulating proteins using genome-wide association  
125 studies (GWAS) for detection of protein quantitative trait loci (pQTL), some of which are referenced  
126 here<sup>3,4,7-9</sup>.

127 Here, we present a genome-wide meta-analysis of 90 cardiovascular-related proteins, many of which  
128 are established prognostic biomarkers or drug targets, measured using the Olink Proximity Extension  
129 Assay CVD-I panel<sup>10</sup> in 30,931 subjects across 14 studies. The identified pQTLs were combined with  
130 other sources of information to suggest new target candidates underpinned by insights into *cis*- and



131 *trans*-regulation of protein levels and to evaluate past and present efforts to therapeutically modify  
132 the proteins analysed in the present investigation. We also show that protein-centric polygenic risk  
133 scores (PRS) can predict a substantial fraction of inter-individual variability in circulating protein  
134 levels, explaining a proportion of disease susceptibility attributable to specific biological pathways.  
  
135 These are the first results to emerge from the SCALLOP consortium, a collaborative framework for  
136 pQTL mapping and biomarker analysis of proteins on the Olink platform ([www.scallop-](http://www.scallop-consortium.com)  
137 [consortium.com](http://www.scallop-consortium.com)).

## 138 Results

### 139 Genome-wide meta-analysis of 90 proteins reveals 467 independent genetic loci 140 associated with plasma levels of 85 proteins

141 Ninety proteins in up to 21,758 participants from 13 cohorts passed quality control (QC) criteria and  
142 were available for GWAS meta-analysis [Supplementary Table 1]. We found a total of 401 pQTLs that  
143 were significant at a discovery  $P$ -value threshold conventional for GWAS ( $P < 5 \times 10^{-8}$ ) [Figure 1]  
144 [Supplementary Table 2]. Conditioning each of these primary pQTLs using the GCTA-COJO software,  
145 we identified an additional 144 proximal pQTLs that independently surpassed conventional genome-  
146 wide significance ( $P < 5 \times 10^{-8}$ ), termed as secondary pQTLs. We attempted to replicate the primary and  
147 secondary pQTLs in two independent studies (9,173 participants) whereupon the discovery and  
148 replication datasets were meta-analysed, leading to 315 primary pQTLs and 136 secondary pQTLs  
149 surpassing a Bonferroni corrected  $P$ -value ( $P < 5.6 \times 10^{-10}$ ). The discovery  $P$ -values were used for pQTLs  
150 absent in the replication dataset ( $n_{\text{snp}}=25$ ) [Supplementary Table 2].

151 Some proteins such as SCF, RAGE, PAPP A, CTSL1 and MPO showed association with more than nine  
152 primary pQTLs, but most proteins (22 of 85) were associated with 2 primary pQTLs. We also observed  
153 that some proteins were associated with multiple conditionally significant (secondary) pQTLs such as  
154 CCL-4 with 4 secondary signals, implicating complex genetic regulation of circulating CCL-4 at the  
155 *CCL4* locus.

156 **Analysis of *trans*-pQTLs suggests common mechanisms by which genetic variants**  
157 **affect plasma protein levels**

158 A “best guess” causal gene for each of the CVD-I *trans*-pQTLs was assigned by a hierarchical approach  
159 based on analysis of protein-protein interactions (PPI), literature mining, genomic distance to gene  
160 and manual review of literature around the gene as well as the genomic context of the association  
161 signal. In total, 326 primary *trans*-pQTLs were assigned to unique genes and 30 *trans*-pQTLs were  
162 assigned more than one gene, with *ABO*, *ST3GAL4*, *JMJD1C*, *SH2B3*, *ZFPM2* showing association with  
163 the levels of five or more CVD-I proteins [Extended Figure 2A and 2B] [Supplementary Table 2].

164 Extending this analysis to pQTLs from literature expanded the list of genes with five or more protein  
165 associations to include also *KLKB1*, *GCKR*, *FUT2*, *TRIB1*, *SORT1* and *F12* [Supplementary Table 4].

166 Gene ontology (GO) analysis of genes assigned to all significant *trans*-pQTLs showed functional  
167 enrichment for chemokine binding, glycosaminoglycan binding, receptor binding and G-protein  
168 coupled chemoattractant activity [Figure 2C]. A broader classification of genes assigned to both *cis*-  
169 and *trans*-pQTLs [Figure 2A, 2B] [Supplementary Table 2] using a wider set of tools (Online Methods)  
170 suggested that transcriptional regulation, post-translational modifications, such as glycation and  
171 sialylation, cell-signalling events, protease activity and receptor binding are potential common  
172 mechanisms by which *trans*-pQTLs influence circulating protein levels. The default gene calls and  
173 paths for the CVD-I *trans*-pQTLs based on PPI and literature mining can be visualised using the  
174 [SCALLOP CVD-I network tool](#) [Extended Figure 2C] whereas details on the classification of genes are  
175 available in the Online Methods, [Supplementary Information 1] and [Supplementary Table 3].

176 **Evidence of mRNA expression mediating associations with a third of *cis* pQTLs**

177 We investigated the overlap of the CVD-I *cis*- and *trans*-pQTLs with expression quantitative trait loci  
178 (eQTL) by a combination of approaches and eQTL studies, including direct genetic lookups and co-  
179 localisation using PrediXcan<sup>11</sup> and SMR / HEIDI<sup>12</sup>. For direct lookups, three studies were used:  
180 LifeLines-DEEP (whole blood), eQTLGen meta-analysis (whole blood and PBMCs) and GTEx (48 tissue  
181 types). Of 545 pQTLs from [Supplementary table 2], eQTL data were available for 434 SNP-transcript

182 pairs, including 168 *cis*-pQTLs and 266 *trans*-pQTLs. Of these, 72 (43%) of *cis*-pQTLs had at least one  
183 corresponding eQTL (FDR<0.05) in any of the eQTL datasets investigated, implicating 42 of the 75  
184 proteins with a *cis*-pQTL. At a more stringent eQTL p-value of  $P < 5 \times 10^{-8}$ , the percentage with a  
185 corresponding eQTL was 26 %, similar to some previous reports<sup>13-15</sup> [Supplementary Table 5].

186 Co-localisation analysis of CVD-I *cis*-pQTLs and mRNA levels was performed in selected tissues from  
187 the GTEx project by first imputing mRNA expression of the CVD-I protein-encoding transcripts using  
188 the PrediXcan<sup>11</sup> algorithm in one of the SCALLOP CVD-I cohorts (IMPROVE), and then testing imputed  
189 mRNA levels for association with CVD-I plasma protein levels using linear regression. Twenty-six of  
190 the 90 CVD-I proteins were associated with their corresponding mRNA transcript (FDR<0.05) in at  
191 least one of the 20 GTEx tissues investigated [Extended Figure 3]. All 26 proteins were among the 42  
192 proteins found to also be an eQTL by direct lookups. Proteins CCL4, CD40, CHI3L1, CSTB and IL-6RA all  
193 associated with their corresponding transcript across five or more tissues whereas proteins ST2 and  
194 RAGE showed significant association exclusively in lung, and CTSD exclusively in skeletal muscle.

195 To further investigate if the CVD-I protein pQTLs overlap with eQTLs, we used the SMR/HEIDI  
196 methods<sup>12</sup>, using data from the Consortium for the Architecture of Gene Expression (CAGE) study.  
197 SMR/HEIDI tests the hypothesis that there is a single variant affecting protein and gene expression  
198 (pleiotropy or causality), with the alternative hypothesis being that protein and gene expression are  
199 affected by two distinct variants. In total, 125 associations between 96 genes and 54 proteins were  
200 identified at an experiment-wise SMR test significance level ( $P_{SMR} < 0.05/8558$ ) and a stringent HEIDI  
201 test threshold ( $P_{HEIDI} > 0.01$ ) [Supplementary Table 6], of which 23.2 % were in *cis*-pQTL regions, such  
202 as IL-8 and U-PAR. The 96 genes were located in 74 loci, suggesting that pleiotropic associations  
203 between protein and mRNA expression were present for 18.4 % of significant and suggestive primary  
204 loci using SMR / HEIDI.

205 **A minor proportion of *cis*-acting pQTLs are in high linkage-disequilibrium with**  
206 **non-synonymous coding variants**

207 “Pseudo-pQTLs” caused by epitope effects, i.e. differential assay recognition depending on presence  
208 of protein-altering variants, is a theoretical possibility for *cis*-pQTLs and likely dependent on the  
209 method of protein quantification<sup>4,16</sup>. To evaluate the potential for pseudo-pQTLs among the CVD-I  
210 pQTLs, we investigated presence of protein-altering variants for sentinel variants or variants in high  
211 linkage disequilibrium with a sentinel variant. Of the 90 proteins, 85 had at least one pQTL, including  
212 12 with only *cis*-pQTLs, 10 with only *trans*-pQTLs and 63 with both *cis*- and *trans*-pQTLs. Of the 170  
213 primary or secondary *cis*-pQTLs for 75 proteins, 20 *cis*-pQTLs for 18 proteins had a sentinel variant in  
214 high linkage disequilibrium (LD;  $R^2 > 0.9$ ) with a protein-altering variant, which suggests potential to  
215 affect assay performance [Supplementary Table 2].

216 **Orthogonal evidence supports causal gene to protein relationships for a subset of**  
217 **the CVD-I *trans*-pQTLs**

218 Of the 326 *trans*-pQTLs identified, eight were assigned to gene products targeted by compounds or  
219 antibodies that have been in clinical development [Supplementary Table 7]. Assuming that *trans*-  
220 pQTLs represent causal relationships between gene variants and proteins, we hypothesized that the  
221 downstream CVD-I proteins associated with CVD-I *trans*-pQTL genes would be modulated on  
222 therapeutic modification of the gene product. Support for this hypothesis was obtained by previous  
223 work showing that circulating FABP4 is upregulated upon treatment with glitazones (PPARG  
224 inhibitors)<sup>17</sup>; that circulating IL-6 is increased after treatment with tocilizumab<sup>18</sup> (IL6R inhibitor) and  
225 that circulating TNF-R2 is decreased upon infliximab (TNFA inhibitor) treatment in patients with  
226 Crohn’s disease<sup>19</sup>, which supports CVD-I *trans*-pQTLs for these proteins. Along these lines, we present  
227 novel evidence from a clinical trial supporting our observations that a CCR5 variant is a *trans*-pQTL  
228 for plasma CCL-4 and a variant in CCR2 is a *trans*-pQTL for plasma MCP-1 [Supplementary table 2].  
229 CCR5 and CCR2 are targeted in combination by the small-molecule dual-inhibitor PF-04634817<sup>20</sup>. To  
230 test whether dual inhibition of CCR5 and CCR2 resulted in a change of circulating CCL-4 and MCP-1  
231 respectively, we measured these proteins in 350 type 2 diabetes patients in a randomized, double-

232 blind, placebo-controlled phase-II trial evaluating the efficacy of PF-04634817 in diabetic  
233 nephropathy (NCT01712061). In addition, we also measured known or suspected ligands of CCR5 and  
234 CCR2, including CCL-3, CCL-5 (RANTES) and CCL-8, and 5 additional proteins that were present on the  
235 Olink CVD-I panel, and for which assays were readily available. Compared to placebo, we observed a  
236 9.25-fold increase in circulating MCP-1 levels ( $p < 0.0001$ ) and a 2.11-fold increase in circulating CCL4  
237 levels ( $p < 0.0001$ ) at week 12 [Figure 3A]. An alternative ligand for CCR-2; CCL-8 did not change  
238 following exposure to PF-04634817, and neither did other CCR-5 ligands, such as CCL-5 (RANTES) and  
239 CCL-3. Moreover, EN-RAGE, FGF-23, KIM-1, myoglobin and TNFR-2 were unchanged following PF-  
240 04634817 exposure [Extended Figure 4]. We conclude that CVD-I *trans*-pQTLs at *CCR5* and *CCR2* were  
241 concordant with the effects of PF-04634817 in human.

242 Two of the genes implicated by CVD-I *trans*-pQTLs, *ABCA1* and *TRIB1* for circulating SCF levels, were  
243 also investigated in the mouse. Mice with liver-specific or whole-body knockdown of *ABCA1*<sup>21</sup> and  
244 *TRIB1*<sup>22</sup> respectively showed decreased plasma levels of SCF compared to matched wild-type controls  
245 [Figure 3B], concordant with the human CVD-I *trans*-pQTLs.

## 246 Mendelian randomization analysis revealed 25 CVD-1 proteins causal for complex 247 traits with strong evidence

248 To identify potential causal disease pathways indexed by proteins, we conducted an MR analysis of  
249 85 proteins across 38 outcomes. 25 proteins showed strong evidence of causality for at least one  
250 disease or phenotype and an additional 24 proteins showed intermediate evidence of causality.  
251 [Figure 4A] [Extended Figure 7] [Supplementary Figure 1]. Using open-source information  
252 ([clinicaltrials.gov](https://clinicaltrials.gov)) ([www.ebi.ac.uk/chembl/](http://www.ebi.ac.uk/chembl/)) ([www.drugbank.ca/](http://www.drugbank.ca/)) ([www.opentargets.org](http://www.opentargets.org)) and  
253 Clarivate Integrity ([integrity.clarivate.com](https://integrity.clarivate.com)), we identified records on past or present clinical drug  
254 development programs for 14 of the 25 proteins, all of which have been in phase 2 trials or later  
255 [Supplementary Table 7]. Of the 14 proteins, seven proteins were targeted for an indication different  
256 from the phenotype implicated by our MR analysis. Eleven of the 25 proteins have never been

257 targeted in clinical trials, but may provide new promising target candidates for indications closely  
258 related to the traits in the MR analysis.

259 Several published MR findings were confirmed, including that *IL6RA* variants associated with higher  
260 circulating levels of interleukin-6 (IL-6) and soluble IL6-RA were associated with lower risk of coronary  
261 heart disease (CHD), rheumatoid arthritis (RA) and atrial fibrillation but higher risks of atopy, such as  
262 asthma and eczema<sup>23</sup>. We also replicated previous findings suggesting a causal contribution of IL-1ra  
263 to rheumatoid arthritis (RA) but an inverse causal relationship with cholesterol levels<sup>24</sup>, and a  
264 protective role of genetically higher MMP-12 against stroke<sup>4,25</sup>.

265 Some novel MR observations included higher levels of CD40 protein and increased risk of RA, higher  
266 MMP-12 and increased risk of eczema, and higher TRAIL-R2 proteins levels and prostate cancer.  
267 Further, Dkk-1 has been targeted by a humanised monoclonal antibody (DKN-01) in clinical trials for  
268 advanced cancer (NCT01457417, NCT02375880), and was in our study causally linked to higher risk of  
269 bone fractures and lower risk of estimated bone mineral density (eBMD). In addition, strong  
270 evidence for protective roles of PLGF in CHD, CASP-8 in breast cancer and ST2 in asthma was  
271 observed. RAGE was causally linked to several traits, including lower body mass index (BMI) and a  
272 corresponding lower risk of type 2 diabetes (T2D), higher total cholesterol and triglycerides and  
273 higher risk of prostate cancer and schizophrenia. A small molecule brain penetrant RAGE inhibitor  
274 was tested in a phase 2 trial of Alzheimer's disease (NCT00566397), but was stopped early for futility.  
275 We saw no strong signal for Alzheimer's disease (or vascular disease) in our MR analysis. Our findings  
276 identify potential target-mediated effects across multiple other complex phenotypes that might  
277 manifest in beneficial and/or harmful effects on patients receiving RAGE-modifying therapies.

278 We also collated observational evidence for 23 of the 50 protein-trait pairs identified as causal in the  
279 MR analysis [supplementary table 10]. The direction of effect inferred from observational studies was  
280 concordant with the effect direction from MR estimates for 12 pairs.

281 **Heritability analysis and polygenic risk scores (PRS) demonstrates large**  
282 **differences in genetic architecture**

283 We calculated SNP-heritability contributed by the major reported loci (major loci  $h_{\text{SNP}}^2$ , any pQTL  
284 included in [supplementary table 2]), as well as additional genome-wide SNP-heritability (polygenic  
285  $h_{\text{SNP}}^2$ ) for each protein included in the entire SCALLOP CVD-I meta-analysis. We observed a large  
286 range of different genetic architectures: Differences in magnitude of the genetic component ( $h_{\text{SNP}}^2$ )  
287 ranged from 0.01 (EGF) to 0.46 (IL-6RA). Differences in the contribution from non-genome-wide  
288 significant SNPs ranged from essentially monogenic (e.g. IL-6RA) to others showing considerable  
289 locus heterogeneity with genetic contributions originating entirely from a polygenic background with  
290 no single dominating locus (e.g. PDGF-B and Galanin) [Figure 5].

291 In addition, we calculated the out of sample variance explained in the independent Malmo Diet and  
292 Cancer (MDC) study (N=4,678) both for genome-wide significant loci (major loci  $V.E._{\text{PRS}}$ ), as well as  
293 additional variance explained by adding PRS (polygenic  $V.E._{\text{PRS}}$ ) [Figure 5]. The protein PRS' applied in  
294 the MDC study for 11 proteins exceeded 10 % of variance explained ( $V.E._{\text{PRS}}$ ) and the PRS' for another  
295 14 proteins exceeded 5 % of variance explained, suggesting that the genetic contribution to inter-  
296 individual variability of CVD-I protein levels is considerable.

297 **A polygenic risk score for circulating ST2 levels shows a dose-response**  
298 **relationship with asthma**

299 Since circulating ST2 showed strong evidence of causation in asthma and inflammatory bowel disease  
300 (IBD) and the polygenic  $V.E._{\text{PRS}}$  model for ST2 explained nearly 20 % of its variance, we attempted to  
301 quantify the effect of the ST2 polygenic  $V.E._{\text{PRS}}$  on circulating ST2 levels in the MDC study, and risk of  
302 asthma and IBD in 337,484 unrelated White British subjects in the UK Biobank. The range of  
303 circulating ST2 across 11 categories of the ST2 PRS in MDC was nearly 1.2 standard deviations [Figure  
304 6A]. Corroborating the Mendelian randomization analysis, the ST2 PRS showed a strong negative  
305 dose-response relationship with risk of asthma ( $p=1.2 \times 10^{-8}$ ) and a positive trend for risk of IBD  
306 ( $p=0.13$ ) [Figure 6B and 6C]. Overlaying the linear trends for ST2 levels, asthma and IBD using meta-

307 regression, an increase in the PRS equivalent to a 1 standard deviation higher circulating ST2,  
308 corresponded to a 8.6 % (95%CI 3.8%, 13.2%; P=0.004) reduction in the relative risk of asthma and a  
309 4.3 % (95%CI -3.8%, 13.0%; P=0.263) increase in the relative risk of IBD [extended Figure 8].

### 310 Reverse Mendelian randomization identifies widespread causal relationships, 311 where complex phenotypes affects CVD-I proteins

312 To investigate whether genetic susceptibility (liability) to complex disease and phenotypes causally  
313 alter circulating levels of CVD-I proteins, we also performed MR using 38 complex phenotypes  
314 (including continuous risk factors, such as adiposity and clinical outcomes, such as T2D) as exposure  
315 and CVD-I protein levels as outcomes. All CVD-I proteins were causally altered by at least one  
316 complex phenotype. BMI and estimated glomerular filtration rate (eGFR) causally affected 32 and 29  
317 of the 85 tested proteins respectively [Figure 7A] [Extended Figure 7] [Supplementary Figure 2]. BMI  
318 seemed to causally affect protein levels in both positive and negative directions, whereas only REN  
319 (renin) was causally decreased with genetically higher eGFR. In an effort to elucidate whether these  
320 estimates were recapitulated in simple observational analyses, we compared effect estimates from  
321 linear regression analyses of associations of BMI and eGFR with each respective CVD-I protein in one  
322 of the participating study cohorts (IMPROVE). The correlation between the observational and MR  
323 estimates were high for BMI (R=0.78), and more modest for eGFR (R=0.50) [Figure 7B-C].

## 324 Discussion

325 Using a meta-analysis approach including >30,000 individuals, we identified and replicated 315  
326 primary and 136 secondary pQTLs for 85 circulating proteins to yield new insights for translational  
327 studies and drug development. Our study demonstrates that pQTLs can be harnessed to enhance  
328 evaluation of therapeutic hypotheses for protein targets, and to support those hypotheses with basic  
329 insights into potential protein regulatory pathways and biomarker strategies. However, we also  
330 observed large differences between proteins in relation to genetic architecture, suggesting that the  
331 relative strength to apply these strategies is likely protein-dependent.



332 Our pQTL-based framework was developed to address several key challenges associated with drug  
333 development, including a) mapping of protein regulatory pathways, b) identification of new target  
334 candidates c) repositioning of drugs, d) target-associated safety and e) matching of target  
335 mechanisms to patients by protein biomarkers or genetic PRS' [Figure 8].

336 The mapping of *trans*-pQTLs, which typically have smaller effects on protein levels [Extended Figure  
337 9], was aided by the large SCALLOP discovery sample size, yielding on average 4 independent pQTLs  
338 per protein. A causal gene was assigned for each *trans*-pQTL to generate hypotheses that can be  
339 further tested using *in vitro* or *in vivo* perturbation experiments. The robustness of causal gene  
340 assignments for a few selected *trans*-pQTLs was demonstrated using samples from a randomised  
341 controlled trial testing a dual small-molecular inhibitor of the protein products of assigned genes  
342 (*CCR5*, *CCR2*) and transgenic mice with liver-specific knockdown of assigned genes (*ABCA1*, *TRIB1*).  
343 Although further studies will be needed for orthogonal validation of most of the genes assigned from  
344 the CVD-I *trans*-pQTLs, several of the implicated genes have previously been identified as regulators  
345 of some of the CVD-I proteins including *CASP1*<sup>26</sup>, *NLRC4*<sup>26</sup> and *GSDMD*<sup>27</sup> for IL-18, *FLT1*<sup>28</sup> for PLGF,  
346 *ADAM17*<sup>29</sup> for TNFR1 and *SLC34A1*<sup>30</sup> for FGF-23 [Supplementary Table 2].

347 Further, we attempted to estimate the proportion of pQTLs that were likely to be driven by effects  
348 on mRNA expression, using multiple eQTL approaches and datasets. The lowest estimate was  
349 obtained with SMR/HEIDI, suggesting that 18.4 % of pQTLs were also eQTLs whereas direct look-up  
350 and co-localisation analysis using PrediXcan yielded estimates between 26 % - 29 %. We conclude  
351 that the majority of pQTLs identified for the CVD-I proteins were not explained by eQTLs.

352 Clinical-stage targeting with any drug modality was reported for 35 of the 90 proteins on the Olink  
353 CVD-I panel [Supplementary Table 7]. Our MR analysis identified 11 proteins with causal evidence of  
354 involvement in human disease that have not previously been targeted. Among those, four proteins  
355 were causal for a disease phenotype and did not show strong evidence of inverse causality with  
356 another phenotype (increasing specificity for intended indication), including *CHI3L1* and *SPON1* for

357 atrial fibrillation and PAPPa for type-2 diabetes. Strong causal evidence was also identified for  
358 proteins targeted in phase-2 or later development. The MR evidence was concordant with drug  
359 indications for several protein targets but for some also suggested alternative indications or that  
360 monitoring of target-associated safety might be warranted. Monoclonal antibodies that block the  
361 CD40 ligand binding to CD40 – a critical element in T cell activation – have been shown to have  
362 positive clinical effects in patients with autoimmune diseases; but increased risk of  
363 thromboembolism precluded further clinical development<sup>31</sup>. These observations from clinical trials  
364 are in line with our findings that genetically *lower* levels of CD40 are associated with *lower* risk of RA,  
365 but *higher* risk of stroke. There are ongoing efforts to modify CD40L antibodies to retain efficacy  
366 while avoiding thromboembolism<sup>31</sup>. However, our results suggest that decreasing circulating CD40  
367 levels may have target-mediated beneficial effects on RA risk, while increasing the risk of ischemic  
368 stroke, i.e. that the increased risk of thromboembolism (manifest as stroke) is an on-target adverse  
369 effect. TRAIL-R2 is a key receptor for TRAIL, which has been shown to selectively drive tumour cells  
370 into apoptosis. Therefore, considerable effort to agonise TRAIL-R2 for treating cancers has been  
371 made in the past years<sup>32</sup>. We demonstrated that increased circulating TRAIL-R2 is protective against  
372 prostate cancer, which may suggest that this cancer type should be investigated in clinical trials  
373 evaluating the efficacy of TRAIL-R2 agonists.

374 Biomarkers can be broadly classified as generic biomarkers for disease risk or prognosis, or as  
375 biomarkers reflecting the activity of specific disease processes or biology. Biomarkers that enable  
376 matching of target mechanisms to patient subgroups with greater than average benefit from  
377 treatment are enablers of precision medicine. We showed that CCR2/CCR5 small-molecule inhibition  
378 modulated circulating levels of CCL-4 and MCP-1, which may suggest that *trans*-pQTLs can guide  
379 selection of exploratory biomarkers to monitor the efficacy of target mechanisms. We also identified  
380 multiple complex traits causally affecting circulating protein levels. For example, eGFR and BMI  
381 causally influenced over 1/3 of the CVD-I proteins, suggesting that future biomarker studies should  
382 consider these traits as potential confounders. Moreover, the causal phenotype-to-protein

383 associations may represent pathway-related causality to the complex phenotype of interest; or  
384 alternatively, 'reverse causality' which might pose an opportunity to evaluate implicated proteins as  
385 surrogate biomarkers for efficacy in interventional trials<sup>33</sup>. We found that higher BMI causally  
386 lowered RAGE, while higher circulating levels of RAGE were causally linked to a lower risk of T2D.  
387 Thus, developing a hypothetical therapeutic to increase RAGE might represent a mechanism by  
388 which it is possible to off-set the risk of T2D arising from the global increases in obesity.

389 Protein-centric PRS' may allow stratification of individuals with genetic propensity for high circulating  
390 protein levels. Only 10 % of the protein-centric PRS' explained 10 % or more of the protein variance  
391 in the independent replication cohort, including ST2, a prognostic biomarker for heart failure<sup>34</sup>. ST2  
392 showed evidence of inverse causality in asthma and positive causality in IBD. By constructing a  
393 genome-wide polygenic risk score for ST2 levels from the MDC study, applying it to the UK Biobank  
394 and comparing asthma and IBD prevalence across eleven quantiles of the ST2 PRS, estimated the  
395 magnitude of ST2 increase required to decrease the risk of asthma to similar levels as individuals in  
396 the highest ST2 PRS category. Such use of PRS for proteins may be expanded to other disease  
397 endpoints and may be of use in precision medicine, to guide which patients may obtain most benefit  
398 from drugs that pharmacologically alter individual proteins.

399 In conclusion, our findings provide a comprehensive toolbox for evaluation and exploitation of  
400 therapeutic hypothesis and precision medicine approaches in complex disease. Such approaches  
401 provide an excellent opportunity to rejuvenate the drug development pipeline for new treatments.

402 -

## 403 Acknowledgements

404 Secure computing was supported by NeIC Tryggve, which is the Nordic collaboration for sensitive  
405 data funded by NeIC and ELIXIR nodes of participating countries.

406 Sources of Funding for SMCC, part of the national research infrastructure SIMPLER. We acknowledge  
407 the national research infrastructure SIMPLER (the Swedish Infrastructure for Medical Population-  
408 based Life-course and Environmental Research) for provisioning of facilities and support. SIMPLER

409 receives funding through the Swedish Research Council under the grant no 2017-00644. This study  
410 was also supported by additional grants from the Swedish Research Council (grants no 2017-06100;  
411 no 2015-05997 and no 2015-03257), from the Swedish Research Council for Health, Working Life and  
412 Welfare (FORTE grant no 2017-00721) and Stiftelsen Olle Engkvist Byggmästare (grant no 2017/49)

413 S Lubitz is supported by NIH grant 1R01HL139731 and American Heart Association 18SFRN34250007.

414 The Orkney Complex Disease Study (ORCADES) was supported by the Chief Scientist Office of the  
415 Scottish Government (CZB/4/276, CZB/4/710), a Royal Society URF to J.F.W., the MRC Human  
416 Genetics Unit quinquennial programme “QTL in Health and Disease”, Arthritis Research UK and the  
417 European Union framework program 6 EUROSPAN project (contract no. LSHG-CT-2006-018947). DNA  
418 extractions were performed at the Edinburgh Clinical Research Facility. We would like to  
419 acknowledge the invaluable contributions of the research nurses in Orkney, the administrative team  
420 in Edinburgh and the people of Orkney.

421 MAK is supported by a Senior Research Fellowship from the National Health and Medical Research  
422 Council (NHMRC) of Australia (APP1158958). He also has a research grant from the Sigrid Juselius  
423 Foundation, Finland

424 AB was supported by a Wellcome PhD training fellowship for clinicians (204979/Z/16/Z), the  
425 Edinburgh Clinical Academic Track (ECAT) programme

426 J. G. Smith and the genotyping of MPP-RES was supported by grants from the Swedish Heart-Lung  
427 Foundation (2016-0134 and 2016-0315), the Swedish Research Council (2017-02554), the European  
428 Research Council (ERC-STG-2015-679242), the Crafoord Foundation, Skåne University Hospital, the  
429 Scania county, governmental funding of clinical research within the Swedish National Health Service,  
430 a generous donation from the Knut and Alice Wallenberg foundation to the Wallenberg Center for  
431 Molecular Medicine in Lund, and funding from the Swedish Research Council (Linnaeus grant Dnr  
432 349-2006-237, Strategic Research Area Exodiab Dnr 2009-1039) and Swedish Foundation for  
433 Strategic Research (Dnr IRC15-0067) to the Lund University Diabetes Center.

434 The study of the Lifelines-DEEP cohort is supported by the Netherlands Heart Foundation CVON  
435 grant 2018-27 to JF and AZ, Netherlands Organization for Scientific Research (NWO-Vidi grant  
436 864.13.013 to JF, 016.178.056 to AZ, 917.14.374 to LF, Veni grant 194.006 to DZ, gravitation grant  
437 ExposomeNL to AZ, gravitation 024.003.001 to JF), European Research Council (ERC starting grant  
438 715772 to AZ, 637640 to LF), LF also receives financial support from Onco Institute.

439 We would like to thank Professor John Parks at Wake Forest School of Medicine, Winston-Salem, NC  
440 and Professor Daniel Rader at Perelman School of Medicine at the University of Pennsylvania,  
441 Philadelphia, PA for their kind donations of samples from transgenic mice and controls. This research  
442 has been conducted using the UK Biobank Resource under Application Number 13721.

443

444

445

## 446 Author Contributions

447 La.F, SG, QW, DHH, ÅKH, DVZ, EF, EMD, EI, AM contributed to meta-analysis. La.F, ÅKH, DVZ, YW,  
448 JRG, YC, AC, FM, EF, Lu.F, TQ, RW, HJW, JY, AM contributed to functional analysis. La.F, SG, QW, GDS,  
449 TP, TQ, JY, LW, ASB, MVH, EI, AM contributed to Mendelian randomization. JP, NE, SEB, TB, ADB, St.E,  
450 AK, MAK, SHC, JD, Sö.E, CF, Lu.F, PF, VG, Ch.H, AH, ÅJ, PKJ, LL, CML, SL, EMD, MM, APM, RM, MWN,  
451 OP, BP, EP, JS, PS, UV, HJW, AZ, JÄ, JF, GS, TE, Ca.H, UG, ML, Ag.S, JFW, LW, ASB, EI, AM contributed  
452 to cohort level analysis. BS, LM, AM contributed to mouse experiments. KP, JDG, JL, WZ, AQ, AM  
453 contributed to clinical trials. La.F, ÅKH, An.S, JRG, FM, EF, AI, TW, AM contributed to other  
454 downstream analysis. La.F, SG, ÅKH, GE, CF, OM, KM, PMN, JN, MOM, MS, AM contributed to  
455 replication analysis. La.F, SG, QW, MVH, EI, AM contributed to writing. La.F, SG, QW, ASB, MVH, EI,  
456 AM contributed to project planning. All authors gave final approval to publish.

457

## 458 Competing Interests Statement

459 The other authors declare no competing interests

## 460 References

- 461 1. Chames, P., Van Regenmortel, M., Weiss, E. & Baty, D. Therapeutic antibodies: successes,  
462 limitations and hopes for the future. *Br J Pharmacol* **157**, 220-233 (2009).
- 463 2. Holmes, M.V., Ala-Korpela, M. & Smith, G.D. Mendelian randomization in cardiometabolic  
464 disease: challenges in evaluating causality. *Nat Rev Cardiol* **14**, 577-590 (2017).
- 465 3. Folkersen, L., *et al.* Mapping of 79 loci for 83 plasma protein biomarkers in cardiovascular  
466 disease. *PLoS Genet* **13**, e1006706 (2017).
- 467 4. Sun, B.B., *et al.* Genomic atlas of the human plasma proteome. *Nature* **558**, 73-79 (2018).
- 468 5. Williams, S.A., *et al.* Plasma protein patterns as comprehensive indicators of health. *Nat Med*  
469 **25**, 1851-1857 (2019).
- 470 6. Lehallier, B., *et al.* Undulating changes in human plasma proteome profiles across the  
471 lifespan. *Nat Med* **25**, 1843-1850 (2019).
- 472 7. Enroth, S., Johansson, A., Enroth, S.B. & Gyllensten, U. Strong effects of genetic and lifestyle  
473 factors on biomarker variation and use of personalized cutoffs. *Nat Commun* **5**, 4684 (2014).
- 474 8. Emilsson, V., *et al.* Co-regulatory networks of human serum proteins link genetics to disease.  
475 *Science* **361**, 769-773 (2018).
- 476 9. Melzer, D., *et al.* A genome-wide association study identifies protein quantitative trait loci  
477 (pQTLs). *PLoS Genet* **4**, e1000072 (2008).
- 478 10. Assarsson, E., *et al.* Homogenous 96-plex PEA immunoassay exhibiting high sensitivity,  
479 specificity, and excellent scalability. *PLoS One* **9**, e95192 (2014).
- 480 11. Gamazon, E.R., *et al.* A gene-based association method for mapping traits using reference  
481 transcriptome data. *Nat Genet* **47**, 1091-1098 (2015).
- 482 12. Zhu, Z., *et al.* Integration of summary data from GWAS and eQTL studies predicts complex  
483 trait gene targets. *Nat Genet* **48**, 481-487 (2016).
- 484 13. Sun, W., *et al.* Common Genetic Polymorphisms Influence Blood Biomarker Measurements in  
485 COPD. *PLoS Genet* **12**, e1006011 (2016).
- 486 14. Chick, J.M., *et al.* Defining the consequences of genetic variation on a proteome-wide scale.  
487 *Nature* **534**, 500-505 (2016).
- 488 15. Zhernakova, D.V., *et al.* Individual variations in cardiovascular-disease-related protein levels  
489 are driven by genetics and gut microbiome. *Nat Genet* **50**, 1524-1532 (2018).

- 490 16. Solomon, T., *et al.* Identification of Common and Rare Genetic Variation Associated With  
491 Plasma Protein Levels Using Whole-Exome Sequencing and Mass Spectrometry. *Circ Genom*  
492 *Precis Med* **11**, e002170 (2018).
- 493 17. Cabre, A., *et al.* Fatty acid binding protein 4 is increased in metabolic syndrome and with  
494 thiazolidinedione treatment in diabetic patients. *Atherosclerosis* **195**, e150-158 (2007).
- 495 18. Nishimoto, N., *et al.* Mechanisms and pathologic significances in increase in serum  
496 interleukin-6 (IL-6) and soluble IL-6 receptor after administration of an anti-IL-6 receptor  
497 antibody, tocilizumab, in patients with rheumatoid arthritis and Castleman disease. *Blood*  
498 **112**, 3959-3964 (2008).
- 499 19. Gustot, T., *et al.* Profile of soluble cytokine receptors in Crohn's disease. *Gut* **54**, 488-495  
500 (2005).
- 501 20. Gale, J.D., *et al.* Effect of PF-04634817, an Oral CCR2/5 Chemokine Receptor Antagonist, on  
502 Albuminuria in Adults with Overt Diabetic Nephropathy. *Kidney Int Rep* **3**, 1316-1327 (2018).
- 503 21. Bashore, A.C., *et al.* Targeted Deletion of Hepatocyte Abca1 Increases Plasma HDL (High-  
504 Density Lipoprotein) Reverse Cholesterol Transport via the LDL (Low-Density Lipoprotein)  
505 Receptor. *Arterioscler Thromb Vasc Biol* **39**, 1747-1761 (2019).
- 506 22. Burkhardt, R., *et al.* Trib1 is a lipid- and myocardial infarction-associated gene that regulates  
507 hepatic lipogenesis and VLDL production in mice. *J Clin Invest* **120**, 4410-4414 (2010).
- 508 23. Rosa, M., *et al.* A Mendelian randomization study of IL6 signaling in cardiovascular diseases,  
509 immune-related disorders and longevity. *NPJ Genom Med* **4**, 23 (2019).
- 510 24. Interleukin 1 Genetics, C. Cardiometabolic effects of genetic upregulation of the interleukin 1  
511 receptor antagonist: a Mendelian randomisation analysis. *Lancet Diabetes Endocrinol* **3**, 243-  
512 253 (2015).
- 513 25. Mahdessian, H., *et al.* Integrative studies implicate matrix metalloproteinase-12 as a culprit  
514 gene for large-artery atherosclerotic stroke. *J Intern Med* **282**, 429-444 (2017).
- 515 26. Kaplanski, G. Interleukin-18: Biological properties and role in disease pathogenesis. *Immunol*  
516 *Rev* **281**, 138-153 (2018).
- 517 27. Heilig, R., *et al.* The Gasdermin-D pore acts as a conduit for IL-1beta secretion in mice. *Eur J*  
518 *Immunol* **48**, 584-592 (2018).
- 519 28. Autiero, M., *et al.* Role of PlGF in the intra- and intermolecular cross talk between the VEGF  
520 receptors Flt1 and Flk1. *Nat Med* **9**, 936-943 (2003).
- 521 29. Dri, P., *et al.* TNF-Induced shedding of TNF receptors in human polymorphonuclear  
522 leukocytes: role of the 55-kDa TNF receptor and involvement of a membrane-bound and  
523 non-matrix metalloproteinase. *J Immunol* **165**, 2165-2172 (2000).
- 524 30. Tenenhouse, H.S. & Sabbagh, Y. Novel phosphate-regulating genes in the pathogenesis of  
525 renal phosphate wasting disorders. *Pflugers Arch* **444**, 317-326 (2002).
- 526 31. Xie, J.H., *et al.* Engineering of a novel anti-CD40L domain antibody for treatment of  
527 autoimmune diseases. *J Immunol* **192**, 4083-4092 (2014).
- 528 32. de Miguel, D., Lemke, J., Anel, A., Walczak, H. & Martinez-Lostao, L. Onto better TRAILs for  
529 cancer treatment. *Cell Death Differ* **23**, 733-747 (2016).
- 530 33. Holmes, M.V. & Davey Smith, G. Can Mendelian Randomization Shift into Reverse Gear? *Clin*  
531 *Chem* **65**, 363-366 (2019).
- 532 34. McCarthy, C.P. & Januzzi, J.L., Jr. Soluble ST2 in Heart Failure. *Heart Fail Clin* **14**, 41-48 (2018).
- 533 35. Willer, C.J., Li, Y. & Abecasis, G.R. METAL: fast and efficient meta-analysis of genomewide  
534 association scans. *Bioinformatics* **26**, 2190-2191 (2010).
- 535 36. Yang, J., Lee, S.H., Goddard, M.E. & Visscher, P.M. GCTA: a tool for genome-wide complex  
536 trait analysis. *Am J Hum Genet* **88**, 76-82 (2011).
- 537 37. Yang, J., *et al.* Conditional and joint multiple-SNP analysis of GWAS summary statistics  
538 identifies additional variants influencing complex traits. *Nat Genet* **44**, 369-375, S361-363  
539 (2012).

- 540 38. Tigchelaar, E.F., *et al.* Cohort profile: LifeLines DEEP, a prospective, general population cohort  
541 study in the northern Netherlands: study design and baseline characteristics. *BMJ Open* **5**,  
542 e006772 (2015).
- 543 39. Consortium, G.T., *et al.* Genetic effects on gene expression across human tissues. *Nature* **550**,  
544 204-213 (2017).
- 545 40. Urmo Vösa, e.a. Unraveling the polygenic architecture of complex traits using blood eQTL  
546 metaanalysis. *bioRxiv* **October 19**(2018).
- 547 41. Westra, H.J., *et al.* Systematic identification of trans eQTLs as putative drivers of known  
548 disease associations. *Nat Genet* **45**, 1238-1243 (2013).
- 549 42. Lloyd-Jones, L.R., *et al.* The Genetic Architecture of Gene Expression in Peripheral Blood. *Am*  
550 *J Hum Genet* **100**, 371 (2017).
- 551 43. McRae, A.F., *et al.* Identification of 55,000 Replicated DNA Methylation QTL. *Scientific*  
552 *Reports volume 8, Article number: 17605* (2018).
- 553 44. Bulik-Sullivan, B.K., *et al.* LD Score regression distinguishes confounding from polygenicity in  
554 genome-wide association studies. *Nat Genet* **47**, 291-295 (2015).
- 555 45. Vilhjalmsón, B.J., *et al.* Modeling Linkage Disequilibrium Increases Accuracy of Polygenic Risk  
556 Scores. *Am J Hum Genet* **97**, 576-592 (2015).
- 557 46. Sudlow, C., *et al.* UK biobank: an open access resource for identifying the causes of a wide  
558 range of complex diseases of middle and old age. *PLoS Med* **12**, e1001779 (2015).
- 559 47. Bycroft, C., *et al.* The UK Biobank resource with deep phenotyping and genomic data. *Nature*  
560 **562**, 203-209 (2018).

561

562

## 563 Figure and table legends

564

565 **Figure 1. Chromosomal location of all associations discovered.** Cis-pQTLs are shown in red (bold)  
566 and trans-pQTLs in blue if they are significant at a conventional GWAS significance threshold of  
567  $P < 5 \times 10^{-8}$ . The gene annotations refer to the gene closest to the pQTL. A version of this figure with  
568 only loci selected according to the criteria for Mendelian randomization is available as [Extended  
569 figure 1].

570 **Figure 2. Classification of cis- and trans-pQTL genes.** **A.** The gene ontology label of all cis-pQTL  
571 genes, i.e. the protein-encoding genes. **B.** The gene-ontology label of all best-guess trans-pQTL genes.  
572 **C.** Gene set enrichment analysis of genes assigned to all significant trans-pQTLs, showing the top-  
573 gene sets from the Gene Ontology set Molecular Function.

574 **Figure 3. Clinical trial in humans and knock down experiment in mice corresponds to trans pQTL**  
575 **effects. A)** In humans treated with a small molecule dual-inhibitor of CCR5 and CCR2 (PF-04634817)  
576 the induction of MCP-1 and CCL4, mirrors the observed CVD-I trans-pQTLs. Box plots elements are  
577 according to standards for box-and-whisker diagrams. **B)** In mice, knockdown of ABCA1 or TRIB1  
578 resulted in decreased circulating SCF levels mirroring CVD-I trans-pQTLs for SCF. Shown in the plot  
579 are SCF levels of individual mice represented by circles (wild-type in blue and transgenic mice in red)  
580 and the median level per group. P-value is calculated using a two-sided T-test.

581 **Figure 4. Main findings of Mendelian randomization analysis. A.** Heatmap of Mendelian  
582 randomization analyses of 38 complex traits. ICD-10 chapter of indication and clinical trial stage  
583 indicated for each target **B.** Forest plot showing CVD-I proteins with strong evidence of causality in  
584 the Mendelian randomization analysis. Drug development abbreviations: PC: pre-clinical, Ph1: Phase  
585 1, Ph2: Phase 2, Ph3: Phase 3, post-MA: post-marketing authorisation. ICD-10 chapters of disease: A-  
586 B: infectious and parasitic; C-D: neoplasms; D: blood and immune; E: endocrine, nutritional and  
587 metabolic; F: mental and behavioural; G: nervous system; H: eye, adnexa, ear and mastoid; I:  
588 circulatory system; J: respiratory system; K: digestive system; L: skin and subcutaneous tissue; M:  
589 musculoskeletal and connective tissue; N: genitourinary; O: pregnancy, childbirth, puerperium; P:  
590 perinatal; Q: congenital, deformations and chromosomal; R: clinical and lab findings; S-T: injury,  
591 poisoning; U: provisional assignment (new diseases unknown aetiology); V-Y: external causes; Z:  
592 health status & health services

593 **Figure 5. SNP heritability and variance explained by genetics. A.** SNP-Heritability in the SCALLOP  
594 consortium discovery cohorts stratified by contributions major loci (light red) and polygenic effects  
595 (dark red). In the independent MDC cohort, additional variability explained by adding major loci (light  
596 blue) and polygenic risk scores (dark blue). Significance was reported according to the LDSC algorithm  
597 (blue) or a linear regression model (red). **B.** Differences in how protein levels are affected by



598 polygenic (non-genome-wide significant) loci vs major loci, shown for both the SCALLOP consortium  
599 discovery cohorts as  $h_{\text{SNP}}^2$  and for the MDC cohort as variability explained.

600 **Figure 6. Mendelian randomization using polygenic risk scores. A.** Association of a polygenic risk  
601 score (PRS) with ST2 levels in the independent MDC cohort. **B.** Association of the ST2 PRS with  
602 asthma in the UK-biobank. **B.** Association of the ST2 PRS with inflammatory bowel disease (IBD) in  
603 the UK-biobank. The ST2 PRS was divided into 11 quantiles, with the middle group (quantile number  
604 6) as the reference category. Effect estimates are presented as quantile-specific mean differences  
605 (ST2) and odds ratios (asthma and IBD) relative to the reference category.

606 **Figure 7. Mendelian randomization with proteins as outcome. A.** Heatmap showing the causal  
607 estimates of 38 complex traits on CVD-I protein levels. **B.** Correlation between beta-values for  
608 association between body mass index and circulating levels of CVD-I proteins in the IMPROVE cohort,  
609 and causal estimates from the Mendelian randomization analysis of body mass index genetic liability  
610 on same CVD-I proteins. **C.** Same as B but for estimated glomerular filtration rate.

611 **Figure 8. Protein-trait relationships that support target validation, repositioning, target-mediated**  
612 **safety and new candidates for drug development.** For more information, see data presented in  
613 [Supplementary Table 7].

614

615

616

617

618

619

620

621

622

623

624

625

626 **URLs**

627 [www.scallop-consortium.com](http://www.scallop-consortium.com)

628 [www.ebi.ac.uk/gwas/](http://www.ebi.ac.uk/gwas/)

629 [www.proteinatlas.org](http://www.proteinatlas.org)

630 [www.uniprot.org](http://www.uniprot.org)

631 <http://www.pantherdb.org>

632 [david.ncicrf.gov](http://david.ncicrf.gov)

633 [clinicaltrials.gov](http://clinicaltrials.gov)

634 [www.ebi.ac.uk/chembl](http://www.ebi.ac.uk/chembl)

635 [www.drugbank.ca](http://www.drugbank.ca)

636 [www.opentargets.org](http://www.opentargets.org)

637 [neic.no/tryggve/](http://neic.no/tryggve/)

638 **Data availability**

639 The full summary statistics of the Olink CVD-I protein GWAS have been deposited at the [SCALLOP-](#)  
640 [CVD-I online resource](#), allowing access to interactive SCALLOP-CVD-I tools and unrestricted download  
641 access for secondary analyses. Additionally, a full copy has been deposited at  
642 <https://doi.org/10.5281/zenodo.2615265> for long-term retention, as well as with GWAS catalog. A  
643 copy of the polygenic scores have been deposited at the PGS catalog.

## 644 Online Methods

### 645 Selection of proteins

646 Proteins for the Olink PEA CVD-I panel were selected by mining the literature for protein biomarkers  
647 associated with cardiovascular risk or prognosis in human observational studies and in animal models  
648 and by bringing in protein biomarker suggestions from leading cardiovascular disease researchers<sup>10</sup>.  
649 The list of proteins curated from these sources was then pruned down based on availability of high-  
650 quality antibodies and relative abundance of the proteins in human plasma.

651 Intra- and inter-plate coefficients of variation (CV) of the CVD-I panel are available from Olink  
652 Proteomics AB (<https://www.olink.com/resources-support/document-download-center/>). In  
653 addition, we calculated the inter-plate coefficient of variation using data from a pooled plasma  
654 sample in one of the participating cohorts -the IMPROVE study. The mean inter-plate CV was  
655 averaged across proteins was 16.6 %, (range 11 % -26 %) [Supplementary Table 1].

### 656 Cohorts and data collection

657 Summary statistics from GWAS of Olink CVD-I proteins were obtained from 13 cohorts of European  
658 ancestry. The details of all study cohorts are shown in [Supplementary Table 9]. Together the cohorts  
659 included a total of 21,758 individuals; although the average per-protein sample size was 17,747,  
660 since not all proteins passed quality control (QC) in all cohorts. Each cohort provided data imputed to  
661 1000 Genomes Project phase 3 reference or later or to the Haplotype Reference Consortium (HRC)  
662 reference, which resulted in the testing of 21.4M SNPs. Because imputation schemes varied by  
663 cohort, this resulted in an average of 20.3M SNPs under investigation for each protein.

664 Each cohort applied quality control measures for call rate filters, sex mismatch, population outliers,  
665 heterozygosity and cryptic relatedness as documented in [Supplementary Table 8]. Prior to running  
666 the genetic analyses, NPX values of proteins (on the log<sub>2</sub> scale) were rank-based inverse normal  
667 transformed and/or standardised to unit variance, thus avoiding potential Olink batch-differences

668 between cohorts. Genetic analyses were conducted using additive model regressions, with  
669 adjustment for population structure and study-specific parameters [Supplementary Table 8]. Forest  
670 plots of cohort-specific effects are available for all significant and suggestive pQTLs using the [online](#)  
671 [tool](#). Each contributing cohort uploaded the resulting summary statistics in a standardized format  
672 using a secure computational cluster provided by Neic Tryggve (<https://neic.no/tryggve/>). All meta-  
673 analysis was performed in duplicate at two different research centres using completely separate  
674 bioinformatic pipelines (L.F. and S.G.).

### 675 [Data cleaning and meta-analysis](#)

676 A per-protein filtering threshold of >80% samples above the Olink detection limit was applied to each  
677 cohort, leaving data on 90 of the 92 proteins to be analysed. The remaining files had an average of  
678 3% missing samples (per cohort statistics available in [Supplementary Table 8]). Minor allele  
679 frequencies were compared with those reported in 1000 Genomes EUR. A per-SNP filter was applied  
680 based on imputation quality level (at default setting for respective imputation algorithm) and minor  
681 allele count (at least 10 alleles per cohort). This resulted in the omission of 10% of the SNPs. Finally,  
682 meta-analysis was performed using METAL (2011-03-25)<sup>35</sup>, applying the inverse-variance weighted  
683 approach (i.e. the STDERR option). Throughout the manuscript, P-values from this test are reported  
684 as-is, with multiple testing burden handled through appropriate thresholds. *Cis*-pQTLs were defined  
685 as a signal within 1 Mb of the gene encoding the protein and all other signals were defined as *trans*-  
686 pQTLs. See [extended figure 5] for flow chart overview of meta analysis.

### 687 [Replication analyses](#)

688 We sought to replicate the findings in the Malmö Diet and Cancer (MDC) population-based cohort  
689 with 4,678 individuals, and in the Swedish Mammography Cohort Clinical (SMCC, part of the Swedish  
690 national research infrastructure SIMPLER described at [www.simpler4health.se](http://www.simpler4health.se)) population-based  
691 study of 4,495 women. In MDC, genotypes were imputed to the Haplotype Reference Consortium  
692 reference (HRC Unlimited v1.0.1) and data were analysed using linear regression in EPIACTS 3.3.0

693 (linear Wald test). The genotypes in SMCC were measured using Illumina's Global Screening Array  
694 and were imputed up to HRC v1.1 and 1000G phase3 (v5), and linear regressions of rank-based  
695 inverse-normal transformed protein values adjusting for age, storage time, and PC1-15 were  
696 performed using PLINK v2 (4 Mar 2019).

## 697 Conditional and joint association analysis

698 To identify secondary signals at the 401 loci reported in [Supplementary table 2], we performed  
699 analyses conditioning on the primary signal using conditional-joint analysis in GCTA (version 1.26.0)  
700 <sup>36,37</sup>. The Stanley cohort was chosen as an ancestrally well-matched LD-reference cohort. Meta-  
701 analysis summary data were processed with filtering for MAF (0.01) and  $r^2$  ( $<0.001$ ) to ensure that  
702 secondary association signals identified were not driven by LD with the primary signal. See  
703 [Extended figure 6] for a flow chart of signal selection criteria.

## 704 Cross-reference of pQTLs with other complex traits

705 For each pQTL association, we searched PubMed and the EBI GWAS catalogue (URL:  
706 <https://www.ebi.ac.uk/gwas/> : November 2018) for published SNPs with any complex trait within  
707 10kb or having an LD of  $r^2 \geq 0.85$ .

## 708 Comparison between eQTLs and pQTL

709 To identify eQTL that corresponded to each pQTL, we used three independent eQTL studies:  
710 LifeLines-DEEP <sup>38</sup>, GTEx<sup>39</sup> and eQTLGen<sup>40</sup>. Each SNP-protein pQTL pair was first converted to SNP-gene  
711 pairs using Olink platform protein identification and the gene annotation of Ensembl v91. Then, the  
712 significance of eQTLs for these SNP-gene pairs was assessed in three eQTL datasets, using two  
713 different cut-offs: a stringent genome-wide significance threshold ( $P < 5 \times 10^{-8}$ ) and a nominal  
714 significance of  $P < 0.05$ .

715 In the eQTL dataset of LifeLines-DEEP, individual-level whole blood RNA-seq, protein and genotype  
716 data were available. This allowed for a direct comparison of the concordance of blood eQTLs and

717 pQTLs. To do so, we re-tested eQTL associations for all pQTL pairs, using a previously published  
718 pipeline<sup>41</sup>. The resulting eQTLs were considered genome-wide significant if it passed the  
719 permutation-based FDR <0.05 level, or to be nominally significant if the *P*-value was < 0.05.

720 In the eQTL datasets of GTEx v7 and eQTL-Gen, we did not have access to individual level data. Thus,  
721 the comparisons were conducted using publicly available eQTL results. In these datasets, we  
722 considered an eQTL genome-wide significant if it was within the reported genome-wide significant  
723 list, and nominally significant if it had a nominal *P*-value < 0.05. Altogether, if one pQTL pair had at  
724 least one significant eQTL effect in any dataset irrespective of allelic direction it was considered an  
725 overlapping pQTL-eQTL pair.

## 726 Expression SMR analysis

727 We performed an SMR and HEIDI (heterogeneity in dependent instruments) analysis<sup>12</sup> to identify the  
728 expression levels of genes that were associated with protein abundance through pleiotropy using  
729 pQTL summary statistics from this study and cis-eQTL summary data from published studies<sup>42,43</sup>.

730 The eQTL summary data used in the SMR analysis were from the Consortium for the Architecture of  
731 Gene Expression (CAGE), comprising 38,624 normalized gene expression probes and ~8 million SNPs  
732 from 2,765 blood samples. The eQTL effects were in standard deviation (SD) units of expression  
733 levels. We excluded the gene probes in the major histocompatibility complex (MHC) region and  
734 included only the gene probes with at least one cis-eQTL at  $P < 5 \times 10^{-8}$  (a basic assumption of SMR),  
735 resulting in 9,538 gene expression probes.

736 The SMR test uses a SNP instrument (i.e., the top associated eQTL) to detect association between  
737 two phenotypes (i.e., gene and protein in this case). The HEIDI test utilises LD between the SNP  
738 instrument and other SNPs in the cis-region to distinguish whether the association identified by the  
739 SMR test is driven by a set of shared genetic variants between two traits (pleiotropic or causal model)  
740 or distinct sets of variants in LD (linkage model)<sup>12</sup>. Only the associations that surpassed the genome-

741 wide significance level of the SMR test ( $P_{\text{SMR}} < 0.05 / m$  with  $m$  being the number of SMR tests) and  
742 were not rejected by the HEIDI test ( $P_{\text{HEIDI}} > 0.01$ ) were reported as significant.

### 743 **PrediXcan and transcript-wide association of CVD-I protein levels**

744 Imputation of gene expression was performed in the IMPROVE study. After standard quality control,  
745 genotypes were pre-phased using Eagle2, and then subsequently imputed by minimac4 using the  
746 1000 Genomes reference. A filter on RSQ 0.8 and minor allele frequency 0.01 was set on the imputed  
747 genotypes prior to prediction with PrediXcan, which used 44 tissue models based on GTEx v7.

748 Using protein data collected on the CVD-I chip in the same individuals, the associations between  
749 protein levels in plasma and the predicted expression of their respective coding gene across 20  
750 tissues (from the PrediXcan model) were modelled by a linear model in R. False discovery rate were  
751 estimated based on Q-values (using the R package qvalue). In total, 64 genes in one to 18 tissues  
752 were tested for associations between protein levels and predicted expression. Heatmaps were  
753 constructed (using the pheatmap package in R) for any gene with a significant association ( $\text{FDR} < 0.05$ )  
754 in at least one tissue.

### 755 **Systems Biology**

756 Two sets of network analysis were performed, one using the protein-protein interaction (PPI) data  
757 from the inBio Map™ (InWeb\_InBioMap) and one using significant associations from text-mining  
758 (TM). These two networks each had 13,033 and 14,635 nodes, respectively; and 147,882 and 193,777  
759 edges, respectively. In both setups, the shortest path between any of the cis-gene intermediaries to  
760 the protein was identified; altogether 12,436 pairs were compared. Of the 372 trans-pQTL  
761 associations reported in [Supplementary Table 2], 335 associations had both cis-gene intermediaries  
762 and plasma protein in the network allowing their analysis. The likelihood of a path arising by chance  
763 was calculated by permutation sampling, using 1,000,000 random networks were generated with a  
764 conserved degree distribution. A new algorithm was developed for *de novo* random network

765 generation, which generated random networks with a nearly conserved degree distribution in a  
766 feasible time-frame. Further details are available in [Supplementary Information 1].

### 767 [Assignment of cis-intermediary genes](#)

768 To assign the most plausible causal gene for each of the CVD-I trans-pQTLs we applied a hierarchical  
769 approach based on analysis of InWeb\_InBioMap PPI, TM, and genomic distance between gene and  
770 lead variant at each locus. Results were then manually reviewed by literature, gene expression  
771 analysis (proteinatlas.org) and published pQTLs which led to the re-assignment of 52 genes. The  
772 algorithmic gene assignment was overruled or complemented for instances when the assigned gene  
773 was different from the gene assigned by multiple prior studies [Supplementary table 4]. Gene  
774 Ontology analysis of most plausible genes was performed using the DAVID bioinformatics tools and  
775 the GO MF gene set definition, with default settings. The Panther pathway tool, Uniprot and the  
776 Human Protein Atlas were used to classify the genes according to basic functional class (see URLs).

### 777 [Human in-vivo validation of trans-pQTLs](#)

778 PF-04634817 is a competitive dual inhibitor of CCR2 and CCR5 receptors. In the recent B1261007  
779 study, (ClinicalTrials.gov Identifier: NCT01712061), samples were collected from subjects with  
780 diabetic nephropathy and treated with PF-04634817 for 12 weeks. CCL-2 (MCP-1) was measured in  
781 serum by ELISA at Eurofins (The Netherlands). CCL4 (MIP-1b) and CCL-8 were measured in plasma  
782 using Luminex assays (Bio-Rad, Berkeley, CA). CCL5 (RANTES), was measured in plasma as part of a  
783 multi-analyte panel at Myriad Rules Based Medicine (Austin, TX).

### 784 [Mouse in-vivo validation of trans-pQTLs](#)

785 Plasma from transgenic- and matched control mice were randomised on a PCR plate. The samples  
786 included five mice with targeted deletion of hepatocyte ABCA1<sup>21</sup> together with five matched control  
787 mice, three mice with whole-body TRIB1<sup>22</sup> knockdown and three controls and four mice with liver-  
788 specific knockdown of TRIB1 and four matched controls. Protein levels of stem cell factor (SCF) was  
789 measured using the Olink PEA Mouse exploratory panel according to the manufacturer's instruction



790 (Olink Proteomics, Uppsala, Sweden). The plasma levels of SCF were normalised against average  
791 protein concentrations using information on an additional 91 proteins. TRIB1 whole-body and liver-  
792 specific mice were analysed jointly as were the respective wild-type controls. The median plasma  
793 levels of SCF were compared using the Mann-Whitney U test for unpaired samples.

## 794 Mendelian randomization

795 To study the causal effects of the protein on selected disease outcomes, we performed two-sample  
796 Mendelian randomization analyses. We used between-study heterogeneity to guide the instrumental  
797 variable selection. In the presence of between-study heterogeneity ( $P_{het} < 9 \times 10^{-5}$ ), variants had to  
798 surpass a Bonferroni-corrected p-value threshold in discovery ( $P < 5.6 \times 10^{-10}$ ) and show nominal  
799 significance ( $P < 0.05$ ) in the replication studies (9,173 individuals), with directionally concordant beta  
800 coefficients. In the absence of between-study heterogeneity we included variants showing  
801 conventional genome-wide significance ( $P < 5 \times 10^{-8}$ ) in a meta-analysis of the discovery and replication  
802 datasets. From these, we created two sets of instrumental variables (IVs) for each of the 85 proteins  
803 with variants reaching multiple testing-corrected significance in our discovery GWAS: (a) *cis* IVs  
804 including one or more independent variants (LD  $r^2 = 0.001$  within  $\pm 1$ Mb of the transcript boundaries of  
805 the gene encoding the protein); and (b) *pan* IVs including all independent (LD  $r^2 = 0$ ) variants  
806 associated with the protein, i.e. combining *cis* and *trans* pQTLs. The per-allelic beta coefficients from  
807 the main GWAS analyses were used as weights in the IVs. For the outcomes, we obtained the  
808 relevant SNP-to-trait summary statistics from publicly-available GWAS as outcomes [Supplementary  
809 Table 9]. When lead variants from our main GWAS were not available in these summary statistics, we  
810 replaced them with proxies (LD  $r^2 > 0.85$ ). For each individual SNP-protein and SNP-outcome  
811 association, we generated an instrumental variable Wald ratio estimate, with standard errors  
812 obtained using the delta method. When the instrument included more than one SNP, summary IV  
813 estimates were generated by combining individual SNP Wald estimates by inverse-variance weighted  
814 fixed-effect meta-analysis. We report associations with a Benjamini-Hochberg false discovery rate

815 (FDR)  $\leq$  5%, applied separately to summary estimates from *cis*-pQTL and *pan*-pQTL IVs, using pooled  
816 estimates for all 38 diseases. We graded the evidence of causality using a framework outlined in  
817 [Extended Figure 7], using the following categories: strong (*cis*-IV estimate FDR $\leq$  5%); intermediate  
818 (pan-IV estimate FDR $\leq$  5% with: (i) no heterogeneity between *cis*-IV estimate and pan-IV estimate;  
819 and (ii) no evidence of the MR estimate being unduly influenced by a *trans*-pQTL in leave-one-out  
820 analysis); or weak (pan-IV estimate FDR $\leq$  5% but: no *cis*-pQTL IV available; heterogeneity between  
821 *cis*- and all- IVs; or evidence of undue influence by a *trans*-pQTL). Heterogeneity between *pan*-IV and  
822 *cis*-IV estimates were calculated using Cochran's Q tests, with  $P < 0.05$  denoting evidence against the  
823 null hypothesis, and applying a Bonferroni adjustment for multiple testing. Mendelian randomization  
824 was conducted in duplicate by two separate analysts and analyses were performed in Stata  
825 (StataCorp, Texas, USA) version 13.3 using the *mrivests*, *metan* and *multproc* commands and R. Of  
826 the 2437 IV estimates derived using *cis*-pQTL instruments across the 85 proteins and 38 outcome  
827 traits, the IV estimates of 50 protein-to-disease associations met the FDR $\leq$ 5% (corresponding to an  
828 uncorrected  $P \leq 1.1 \times 10^{-3}$ ). Of the 3044 IV estimates composed using all pQTL instruments, 281 IV  
829 estimates met FDR $\leq$  5% (corresponding to  $P \leq 4.7 \times 10^{-3}$ ; [Figure 4A]).

### 830 Heritability analyses

831 We estimated the total SNP-heritability ( $h_{\text{SNP}}^2$ ) for the plasma level of each protein from the summary  
832 statistics of each individual GWAS by summing the contributions from two independent partitions of  
833 the SNPs: primary major loci and polygenic background. We defined the variance explained by  
834 primary major loci (major loci  $h_{\text{SNP}}^2$ ) as the sum of the estimated variance explained ( $2 * \beta^2 * f * (1-f)$ ),  
835 where  $f$  is the minor allele frequency, and owing to the fact that the phenotypic variance has been  
836 standardized across lead SNPs indexing all primary genome-wide significant loci. We used LDSC  
837 regression<sup>44</sup> to estimate the contribution of the polygenic background (polygenic  $h_{\text{SNP}}^2$ ) for each  
838 protein, which we define as the contribution of all loci not indexed by a genome-wide significant lead  
839 SNP. LDSC regression is known to perform poorly when large effect, major genes are present, as it

840 was derived under the assumption of a simple polygenic genetic architecture<sup>44</sup>. To account for this  
841 and avoid double counting the variance explained by major loci through LD surrogates, prior to  
842 estimating the LDSC regression polygenic  $h_{SNP}^2$ , we censored all SNPs within 10 Mb of genome-wide  
843 significant lead SNPs for all primary loci.

#### 844 Polygenic risk score calculation

845 Polygenic risk scores were derived using LDpred algorithm<sup>45</sup>, which adjusts the effect of each SNP  
846 allele for those of other SNP alleles in linkage disequilibrium (LD) with it, and also takes into account  
847 the likelihood of a given allele to have a true effect according to a user-defined parameter, which we  
848 used as all 7 default LDpred-settings, with values from 1 through  $1 \times 10^{-5}$ . The algorithm was directed  
849 to use HapMap3 SNPs that had a minor allele frequency  $>0.05$ , Hardy-Weinberg equilibrium  $P > 1e-05$   
850 and imputation score  $>0.95$ . Variance explained in the independent MDC-study was tested according  
851 to a step-wise model, first including non-genetic covariates, then additional variability explained by  
852 adding SNPs from genome-wide significant SNPs (major loci V.E.<sub>PRS</sub>), and then additional variability  
853 explained by adding the 7 LDpred-derived scores as additional covariates (polygenic V.E.<sub>PRS</sub>).

#### 854 ST2 polygenic risk score for asthma and inflammatory bowel disease in the UK 855 biobank

856 Prior to analysis subjects who were not White British (based on self-reported ancestry in  
857 combination with genetic PCA) in the maximum unrelated subset were filtered out. All bi-allelic SNPs  
858 with MAF  $\geq 1\%$  and MaCH  $rsq \geq 0.8$  were kept. The Z-score transformed LDpred PRS (wt2) for ST2  
859 was calculated as described for MDC in 337,484 White British UK Biobank participants. Association  
860 with asthma and IBD were tested using logistic regression adjusting for age, sex, PC1-10, genotype  
861 batch using either the continuous PRS or the PRS quantile-bins as predictors. The UK Biobank  
862 protocol has been described previously<sup>46</sup> and is available online (<https://www.ukbiobank.ac.uk>). The  
863 genotype quality control (QC), phasing, and imputation was performed centrally and has been  
864 previously described<sup>47</sup>. Outcomes (defined based on self-reported data at baseline and/or the

865 inpatient and death registry [including primary and secondary causes as well as prevalent and  
866 incident disease]) Asthma: Self-reported touchscreen (6152), self-reported nurse interview (20002),  
867 or ICD-10 "J45". Conflicting self-reported results set to missing unless "J45" was reported.  
868 Inflammatory bowel disease: nurse interview (20002) or ICD-10 K50-K52.

### 869 **Meta-regression analysis for ST2 PRS, asthma and IBD**

870 We estimated the per-quantile and per-SD associations of the weighted PRS for ST2 (MDC study) on  
871 risks of asthma and IBD (UK Biobank) by taking the quantile associations with ST2, asthma and IBD  
872 and conducting meta-regression analyses whereby the dependent variable was the quantile-specific  
873 logOR and corresponding SE of asthma or IBD and the independent variable was the quantile specific  
874 beta coefficient for ST2. This was conducted using the "metareg" package in STATA SE v13.1  
875 (Statacorp, USA). Plots from the metaregression are presented in [Extended Figure 8].

### 876 **Observational evidence**

877 Observational evidence for the CVD-I proteins showing strong evidence of causality in Mendelian  
878 randomization was collated from literature or by de-novo analysis in the IMPROVE cohort  
879 [supplementary table 10]. To identify evidence from literature, we searched for the protein name or  
880 aliases in combination with the implicated trait trait/disease in PubMed. For clinical outcome traits,  
881 only those reported as "significant" by the paper were included, and the table provides the  
882 directional information provided. For quantitative outcome traits, standardised betas and p-values  
883 are reported.

884

885

886

887

888

## Consortium author list

889 Lasse Folkersen<sup>1,2\*</sup>, Stefan Gustafsson<sup>3\*</sup>, Qin Wang<sup>4,5\*</sup>, Daniel Hvidberg Hansen<sup>6</sup>, Åsa K Hedman<sup>1,7</sup>,  
890 Andrew Schork<sup>8,9</sup>, Karen Page<sup>10</sup>, Daria V Zhernakova<sup>11</sup>, Yang Wu<sup>12</sup>, James Peters<sup>13</sup>, Niclas Eriksson<sup>14</sup>, Sarah  
891 E Bergen<sup>15</sup>, Thibaud Boutin<sup>16</sup>, Andrew D Bretherick<sup>16</sup>, Stefan Enroth<sup>17</sup>, Anette Kalnapenkis<sup>18</sup>, Jesper R  
892 Gådin<sup>1</sup>, Bianca Suur<sup>19</sup>, Yan Chen<sup>1</sup>, Ljubica Matic<sup>19</sup>, Jeremy D Gale<sup>20</sup>, Julie Lee<sup>10</sup>, Weidong Zhang<sup>21</sup>, Amira  
893 Quazi<sup>10</sup>, Mika Ala-Korpela<sup>4,5,22</sup>, Seung Hoan Choi<sup>23</sup>, Annique Claringbould<sup>11</sup>, John Danesh<sup>13</sup>, George Davey-  
894 Smith<sup>24</sup>, Federico de Masi<sup>6</sup>, Sölve Elmståhl<sup>25</sup>, Gunnar Engström<sup>25</sup>, Eric Fauman<sup>26</sup>, Celine Fernandez<sup>25</sup>, Lude  
895 Franke<sup>11</sup>, Paul Franks<sup>27</sup>, Vilmantas Giedraitis<sup>28</sup>, Chris Haley<sup>16</sup>, Anders Hamsten<sup>1</sup>, Andres Ingason<sup>8</sup>, Åsa  
896 Johansson<sup>17</sup>, Peter K Joshi<sup>29</sup>, Lars Lind<sup>30</sup>, Cecilia M. Lindgren<sup>31,32,23</sup>, Steven Lubitz<sup>33,23</sup>, Tom Palmer<sup>34</sup>, Erin  
897 Macdonald-Dunlop<sup>29</sup>, Martin Magnusson<sup>35,36</sup>, Olle Melander<sup>25</sup>, Karl Michaelsson<sup>37</sup>, Andrew P. Morris<sup>38,39</sup>,  
898 <sup>32</sup>, Reedik Mägi<sup>18</sup>, Michael W Nagle<sup>26</sup>, Peter M Nilsson<sup>25</sup>, Jan Nilsson<sup>25</sup>, Marju Orho-Melander<sup>40</sup>, Ozren  
899 Polasek<sup>41</sup>, Bram Prins<sup>13</sup>, Erik Pålsson<sup>42</sup>, Ting Qi<sup>12</sup>, Marketa Sjögren<sup>25</sup>, Johan Sundström<sup>43</sup>, Praveen  
900 Surendran<sup>13</sup>, Urmo Vösa<sup>18</sup>, Thomas Werge<sup>8</sup>, Rasmus Wernersson<sup>6</sup>, Harm-Jan Westra<sup>11</sup>, Jian Yang<sup>12,44</sup>,  
901 Alexandra Zhernakova<sup>11</sup>, Johan Ärnlöv<sup>45</sup>, Jingyuan Fu<sup>11,46</sup>, Gustav Smith<sup>47</sup>, Tonu Esko<sup>18,23</sup>, Caroline  
902 Hayward<sup>16</sup>, Ulf Gyllenstein<sup>17</sup>, Mikael Landen<sup>42</sup>, Agneta Siegbahn<sup>48</sup>, Jim F Wilson<sup>29,16</sup>, Lars Wallentin<sup>49</sup>, Adam  
903 S Butterworth<sup>13</sup>, Michael V Holmes<sup>50\*</sup>, Erik Ingelsson<sup>51\*</sup>, Anders Mälarstig<sup>1,52\*</sup>

904

\* these authors contributed equally

905

906

1 Department of Medicine, Solna, Karolinska Institute, Sweden

907

2 Danish National Genome Center, Copenhagen, Denmark

908

3 Department of Medical Sciences, Molecular Epidemiology and Science for Life Laboratory, Uppsala University, Uppsala, Sweden

909

4 Systems Epidemiology, Baker Heart and Diabetes Institute, Melbourne, VIC, Australia

910

5 Computational Medicine, Faculty of Medicine, University of Oulu and Biocenter Oulu, Oulu, Finland

911

6 Intomics, Lottenborgvej 26, 2800 Lyngby (Copenhagen), Denmark

912

7 Pfizer Worldwide Research & Development, Cambridge, MA, USA

913

8 Institute of Biological Psychiatry, Mental Health Center Sct. Hans, Mental Health Services Capital Region, Roskilde, Denmark

914

9 Neurogenomics Division, The Translational Genomics Research Institute (TGEN), Phoenix, AZ, USA

915

10 Early Clinical Development, Pfizer Worldwide Research & Development, Cambridge, MA, USA

916

11 University of Groningen, University Medical Center Groningen, Department of Genetics, Groningen, the Netherlands

917

12 Institute for Molecular Bioscience, The University of Queensland, Brisbane, Queensland, Australia

918

13 BHF Cardiovascular Epidemiology Unit, Department of Public Health and Primary Care, University of Cambridge, United Kingdom

919

14 Department of Medical Sciences, Uppsala Clinical Research Center, Uppsala University, Uppsala, Sweden

920

15 Department of Medical Epidemiology and Biostatistics, Karolinska Institutet, Stockholm, Sweden

921

16 MRC Human Genetics Unit, Institute of Genetics and Molecular Medicine, University of Edinburgh, Western General Hospital, Crewe Road, Edinburgh, EH4

922

2XU, Scotland

923

17 Department of Immunology, Genetics, and Pathology, Biomedical Center, Science for Life Laboratory (SciLifeLab) Uppsala, Box 815, Uppsala University, SE-

924

75108 Uppsala, Sweden

925

18 Estonian Genome Center, Institute of Genomics, University of Tartu 51010, Estonia

926

19 Department of Molecular Medicine and Surgery, Solna, Karolinska Institute, Sweden

927

20 Inflammation and Immunology Research Unit, Pfizer Worldwide Research & Development, Cambridge, MA, USA

928

21 Pfizer Global Product Development, Cambridge, MA, USA

929

22 NMR Metabolomics Laboratory, School of Pharmacy, University of Eastern Finland, Kuopio, Finland

930

23 Program in Medical and Population Genetics, Broad Institute, Cambridge, MA, USA

931

24 MRC Integrative Epidemiology Unit, University of Bristol, UK

932

25 Department of Clinical Sciences, Lund University, Skåne University Hospital, Malmö, Sweden

933

26 Internal Medicine Research Unit, Pfizer Worldwide Research & Development, Cambridge, MA, USA

934

27 Lund University Diabetes Center, Department of Clinical Sciences, Malmö, Sweden

935

28 Department of Public Health and Caring Sciences/Geriatrics, Uppsala University, Uppsala, Sweden.

936

29 Centre for Global Health Research, Usher Institute for Population Health Sciences and Informatics, University of Edinburgh, Teviot Place, Edinburgh, EH8

937

9AG, Scotland

938

30 Department of Medical Sciences, Uppsala University, Uppsala, Sweden.

939

31 Big Data Institute at the Li Ka Shing Centre for Health Information and Discovery, University of Oxford, Oxford, United Kingdom.

940

32 Wellcome Centre for Human Genetics, Nuffield Department of Medicine, University of Oxford, Oxford, United Kingdom.

941

33 Cardiovascular Research Center, Massachusetts General Hospital, United States.

942

34 Department of Mathematics and Statistics, University of Lancaster, Lancaster, UK

943

35 Department of Cardiology, Skåne University Hospital Malmö, Malmö, Sweden

944

36 Wallenberg Center for Molecular Medicine, Lund University, Lund, Sweden

945

37 Department of Surgical Sciences, Uppsala University, Uppsala, Sweden

946

38 Division of Musculoskeletal and Dermatological Sciences, University of Manchester, Manchester, UK

947

39 Department of Biostatistics, University of Liverpool, Liverpool, UK

948

40 Department of Clinical Sciences, Clinical Research Center, Lund University, Malmö, Sweden

949

41 Faculty of Medicine, University of Split, Split, Croatia

950

42 Department of Psychiatry and Neurochemistry, Institute of Neuroscience and Physiology, the Sahlgrenska Academy at the University of Gothenburg,

951

Gothenburg, Sweden

952

43 Department of Medical Sciences, Clinical Epidemiology, Uppsala University, Uppsala, Sweden; and The George Institute for Global Health, University of New

953

South Wales, Sydney, Australia

954

44 Institute for Advanced Research, Wenzhou Medical University, Wenzhou, Zhejiang 325027, China

955

45 Department of Neurobiology, Care Sciences and Society (NVS), Division of Family Medicine and Primary Care, Karolinska Institutet, Sweden

956

46 University of Groningen, University Medical Center Groningen, Department of Paediatrics, Groningen, the Netherlands

957

47 Department of Cardiology, Clinical Sciences, Lund University, Skåne University Hospital, Lund, Sweden.

958 48 Department of Medical Sciences, Clinical Chemistry, Uppsala University, Uppsala, Sweden  
959 49 Department of Medical Sciences, Cardiology and Uppsala Clinical Research Center, Uppsala University, Uppsala, Sweden  
960 50 Clinical Trial Service Unit and Epidemiological Studies Unit (CTSU), Nuffield Department of Population Health, University of Oxford, Oxford, United Kingdom.  
961 51 Department of Medicine, Division of Cardiovascular Medicine, Falk Cardiovascular Research Center, Stanford University School of Medicine, 300 Pasteur  
962 Drive, CV 273, Stanford, CA, 94305, USA.  
963 52 Emerging Science & Innovation, Pfizer Worldwide Research & Development, Cambridge, MA, USA  
964

965

966

967

968

969

970

971

972

973

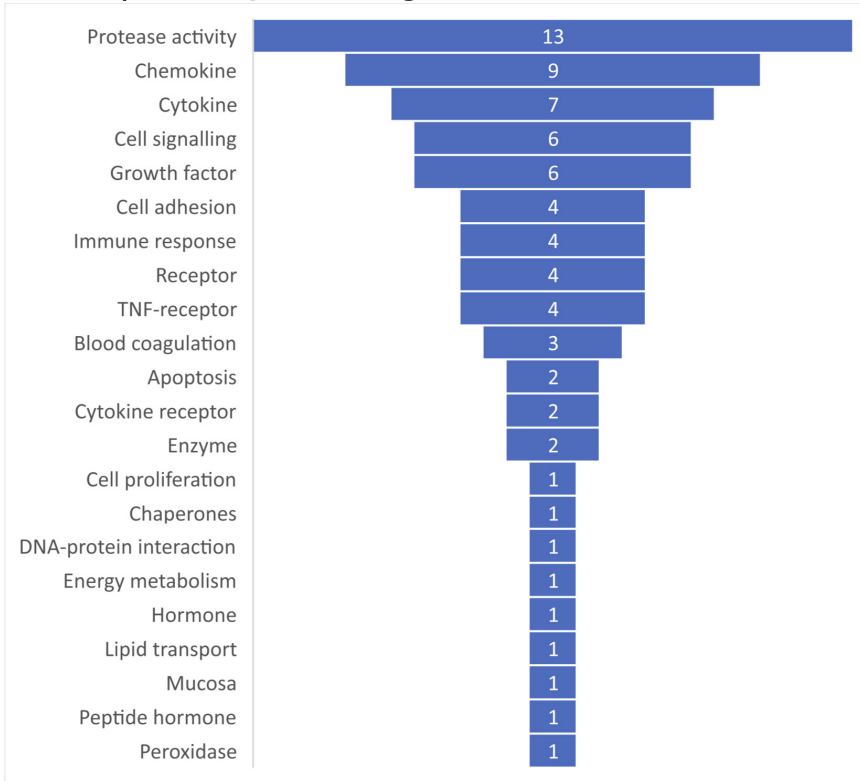
974

975

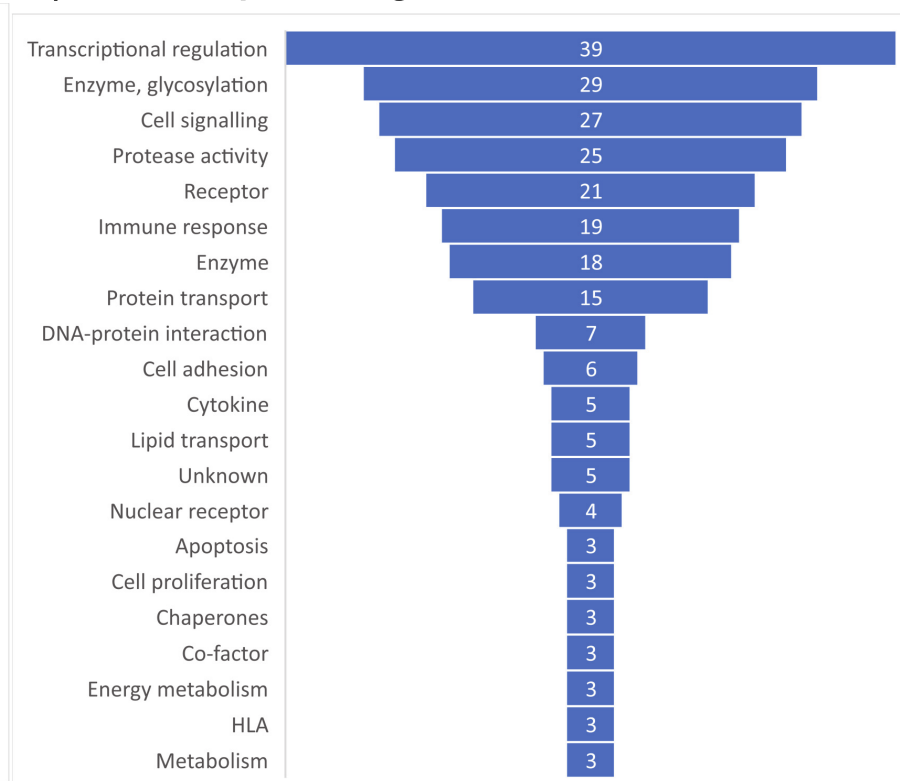
976



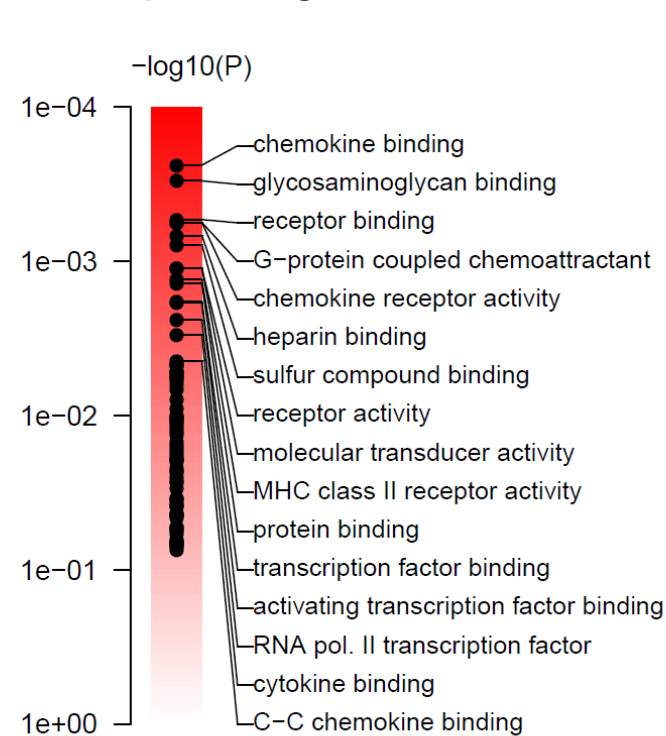
## A) Cis-pQTL genes



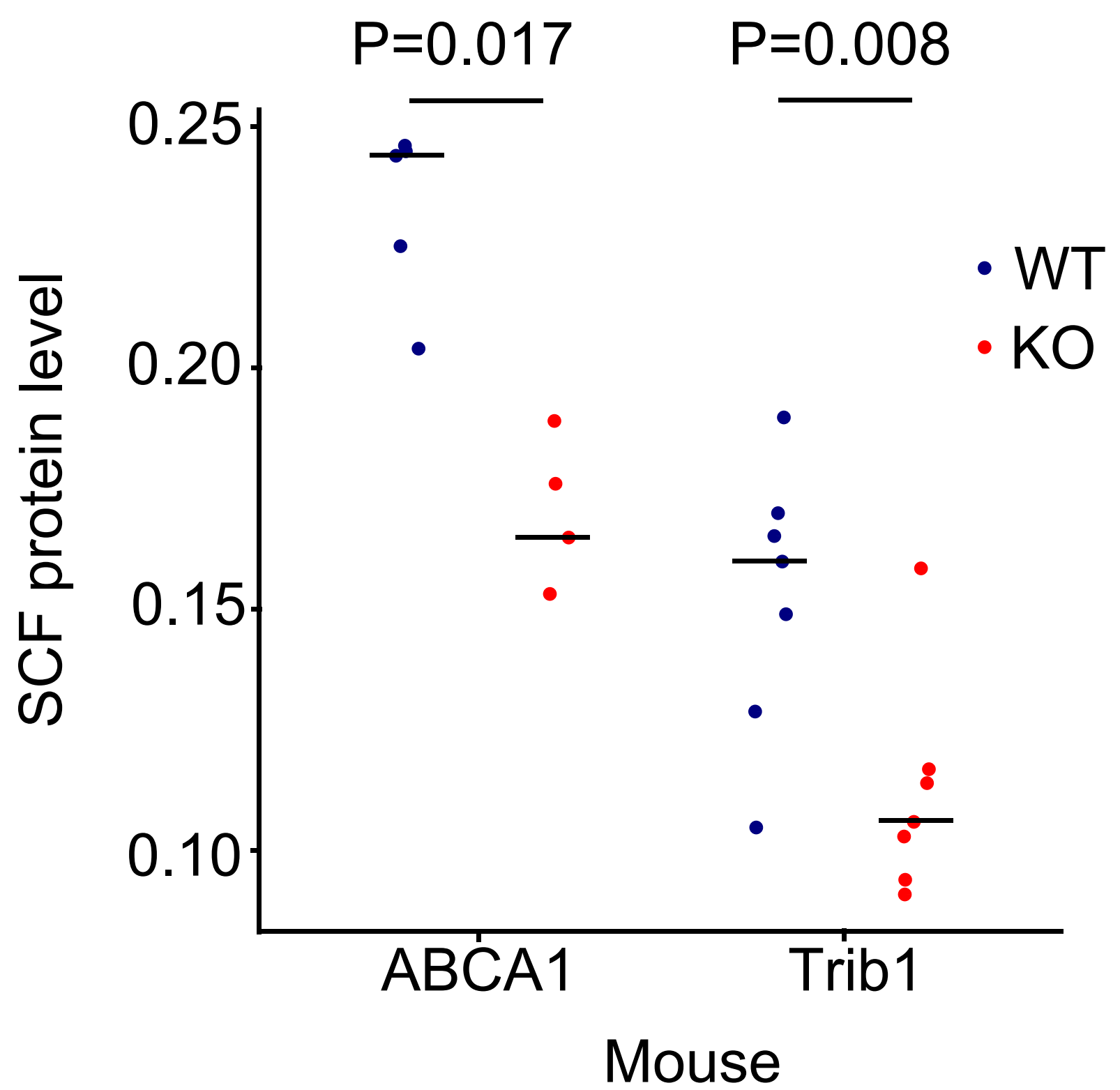
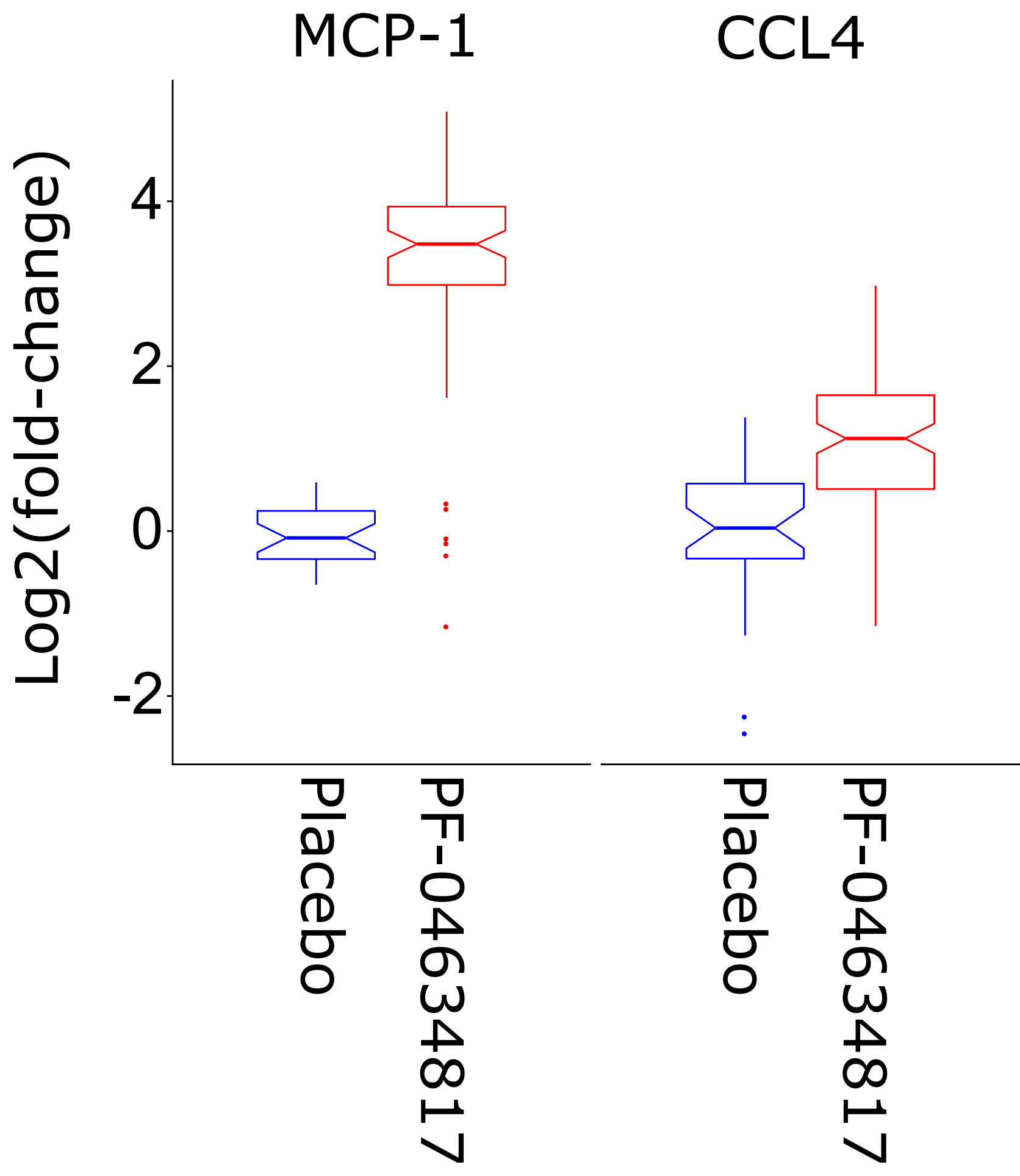
## B) Trans-pQTL genes



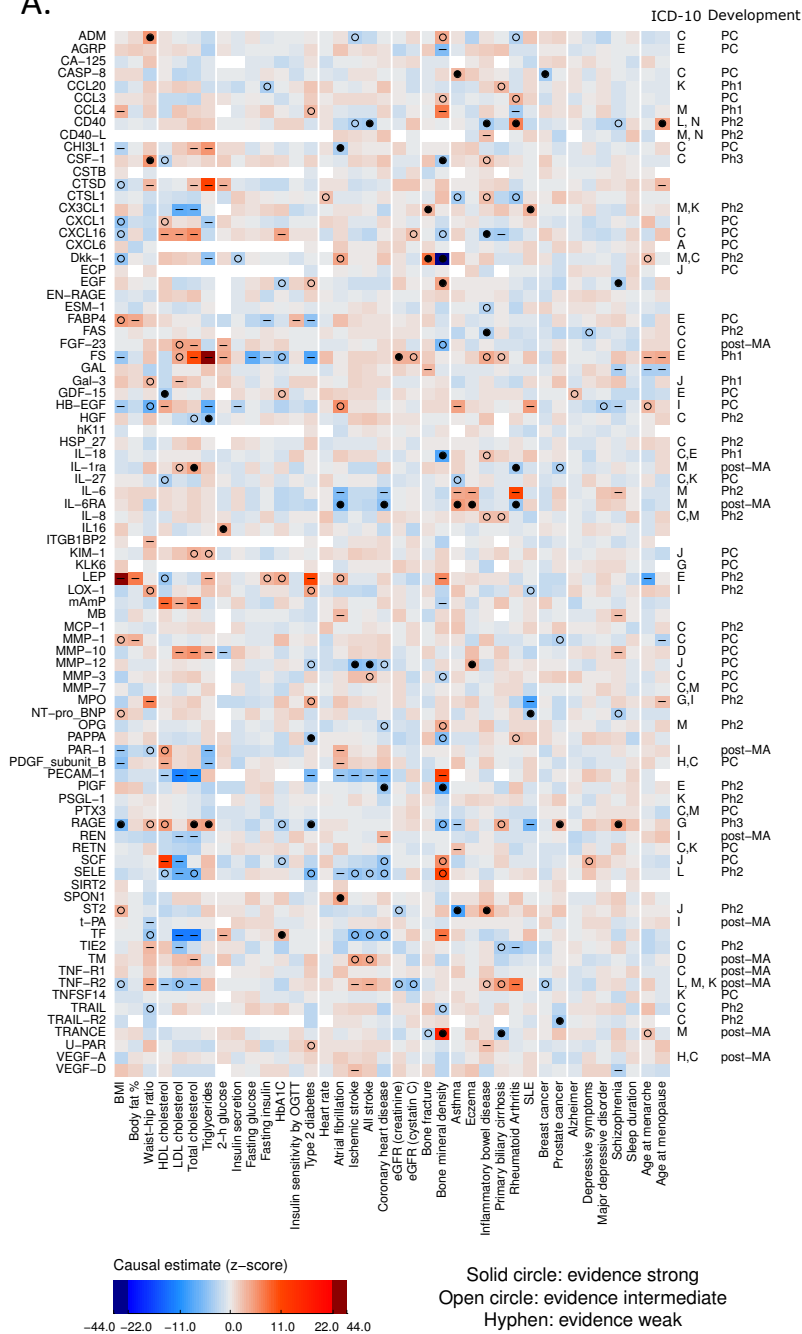
## C) Trans-pQTL genes, enrichment



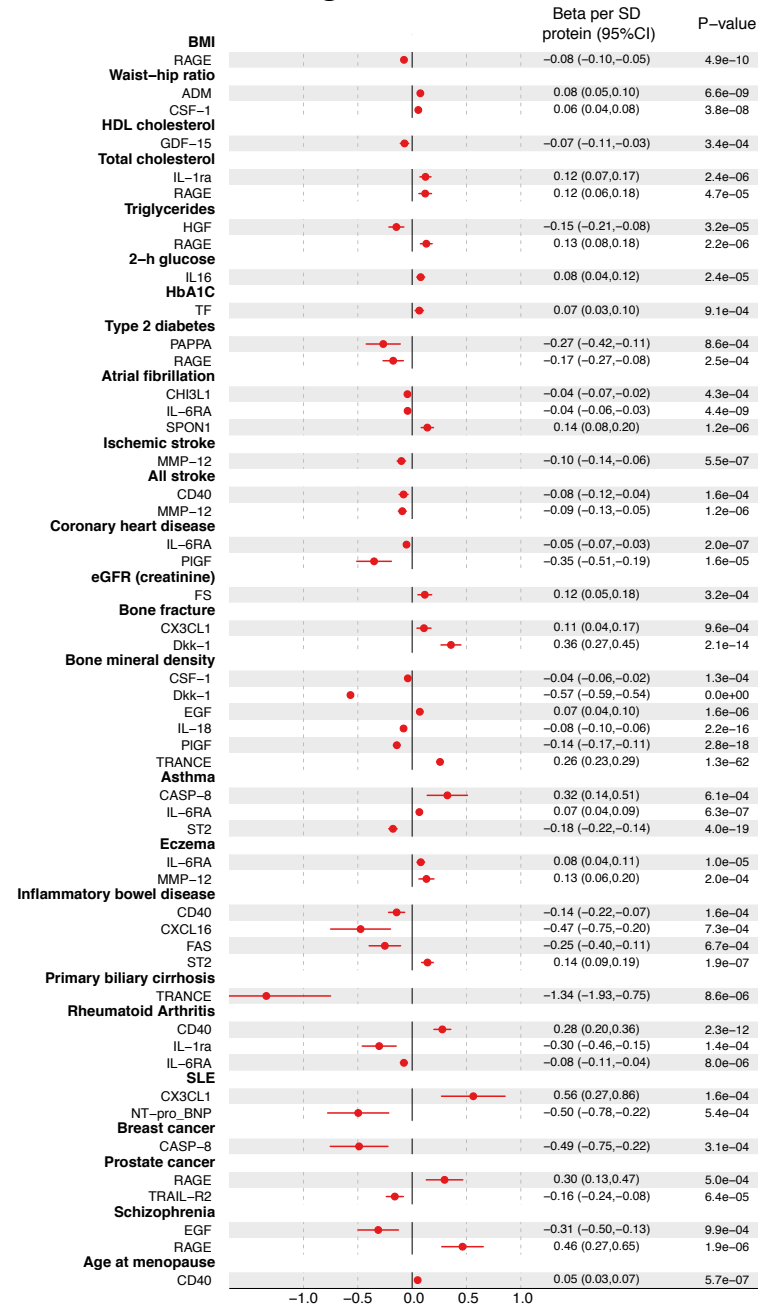




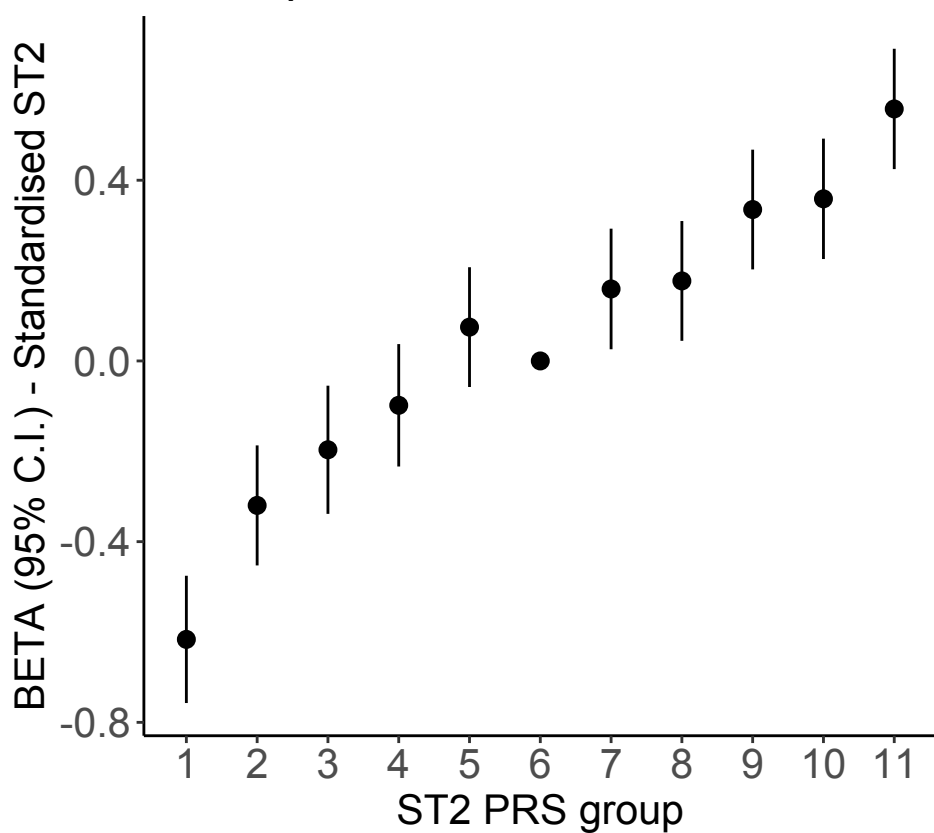
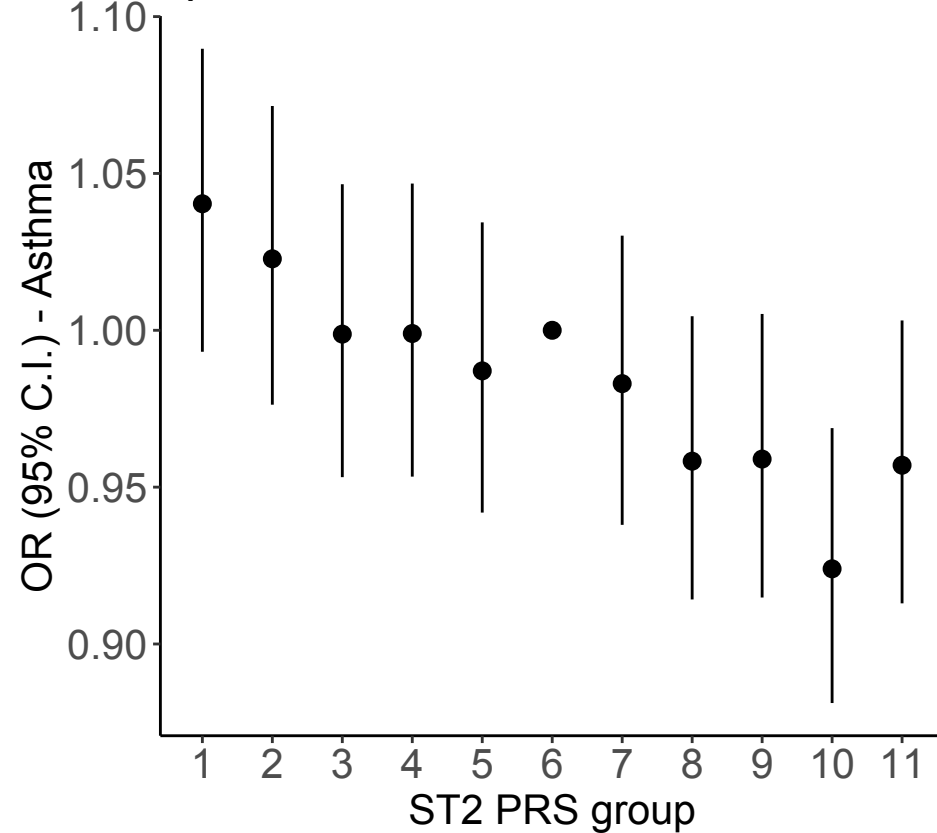
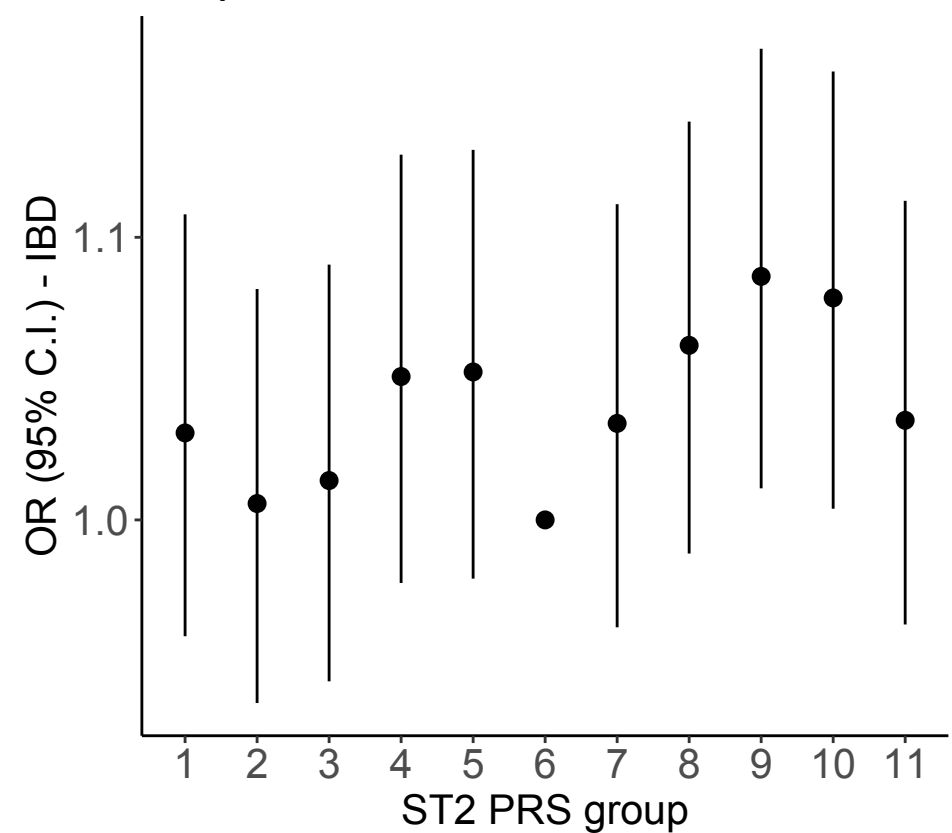
A.



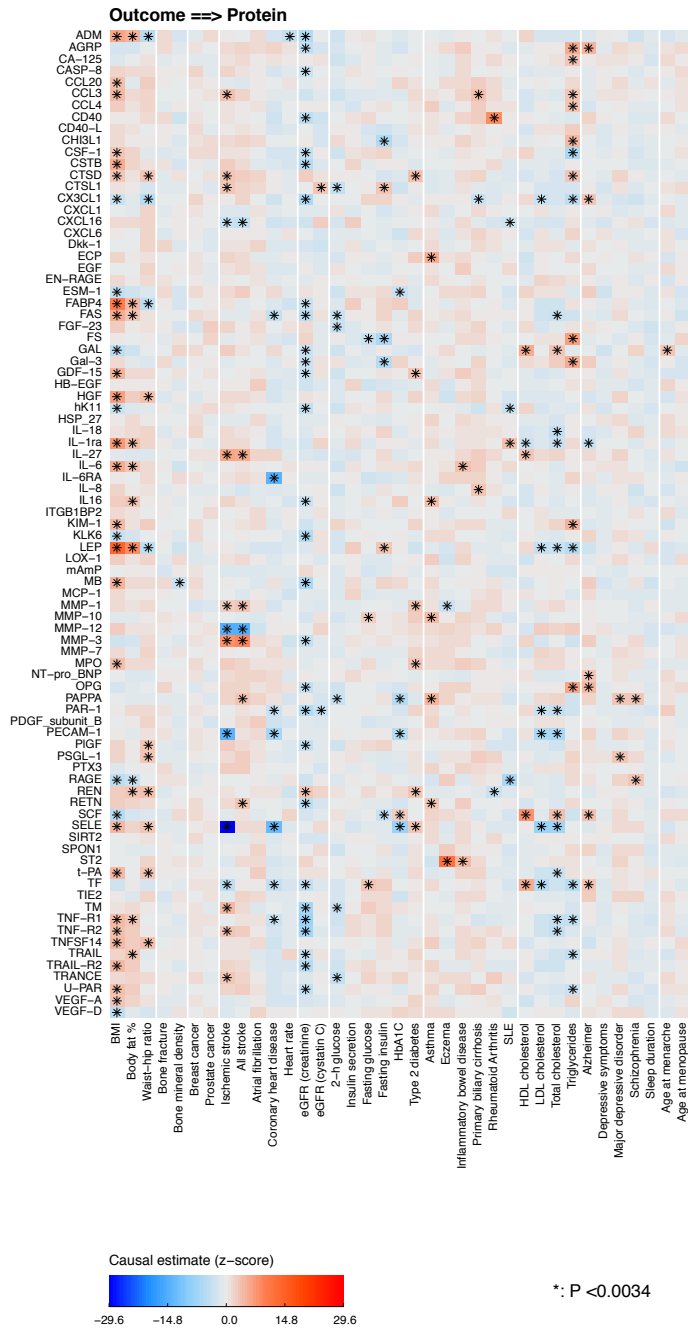
B. MR with strong evidence



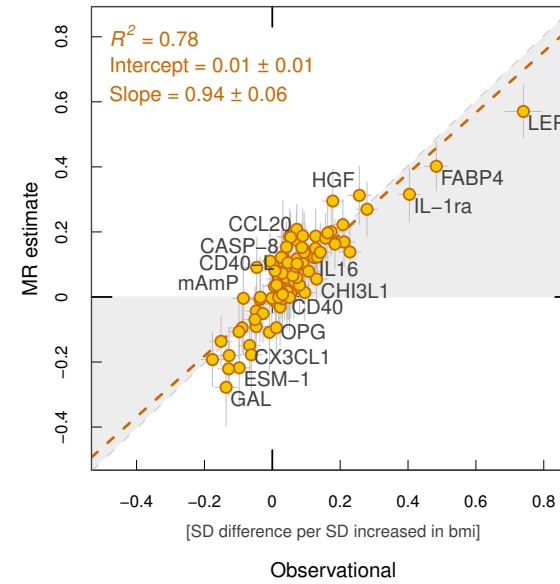


**A) ST2 PRS for ST2 in MDC****B) ST2 PRS for asthma in UK-Biobank****C) ST2 PRS for IBD in UK-Biobank**

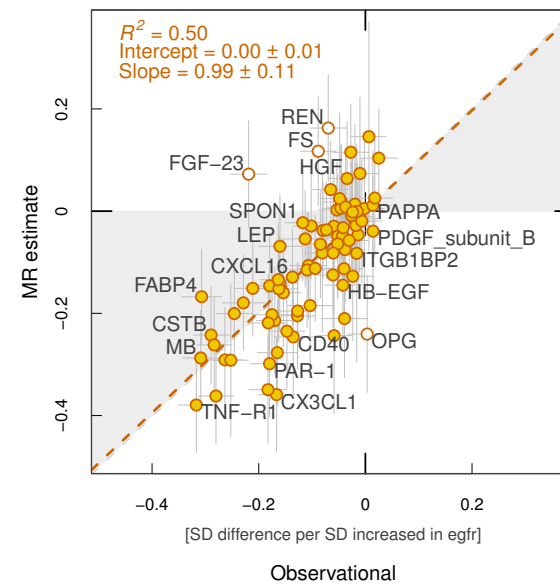
### A. 37 traits to 85 proteins



### B. BMI ==> proteins: MR vs Observational



### C. eGFR ==> proteins: MR vs Observational



### **Target validation**

CASP-8: breast cancer

CD40: IBD, RA

DKK1: eBMD

IL-1RA: RA

IL-6RA: RA, CHD

ST2: asthma

TRAIL-R2: prostate cancer

TRANCE: eBMD

### **New target candidates**

EGF: SCZ, eBMD

IL16: 2h glucose

PAPPA: T2D

SPON1: Afib

TF: HbA1c

### **Repositioning & target-mediated safety**

*(latter denoted by \*)*

ADM: WHR

CASP-8: asthma\*

CD40: stroke\*

CHI3L1: AFib

CSF: WHR, eBMD

CX3CL1: fracture, SLE

CXCL16: IBD

FAS: IBD

GDF-15: HDL-C

HGF: TG

IL-1RA: total cholesterol\*

IL-6RA: asthma, eczema\*

IL-6RA: AFib

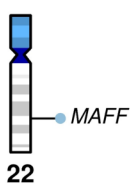
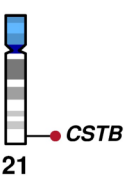
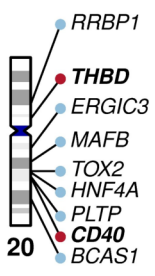
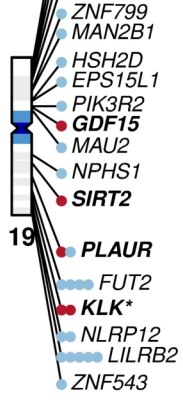
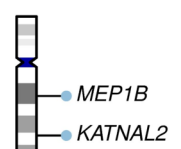
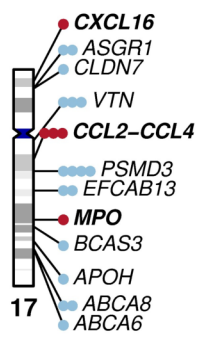
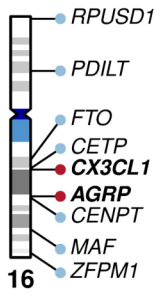
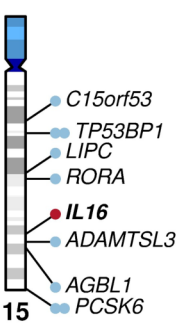
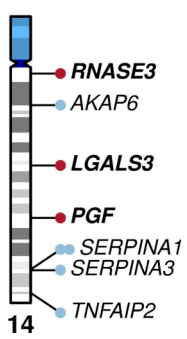
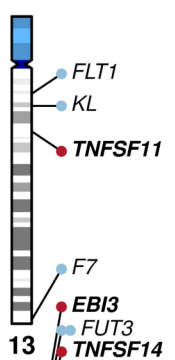
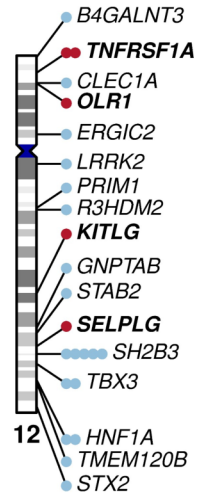
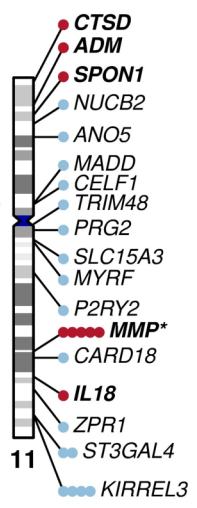
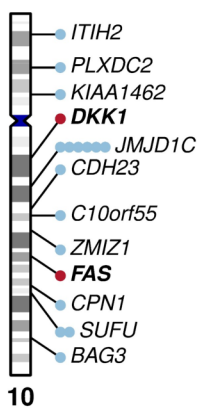
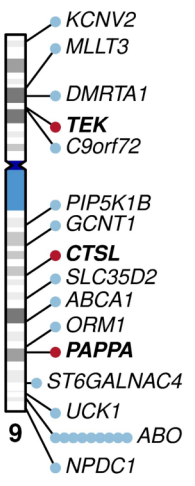
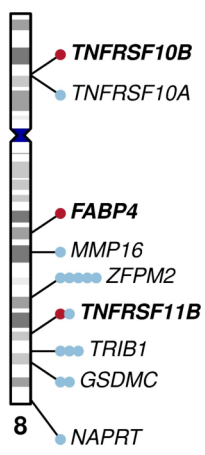
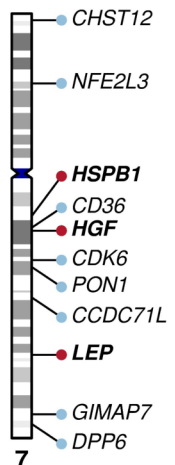
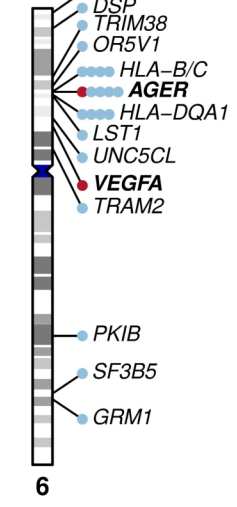
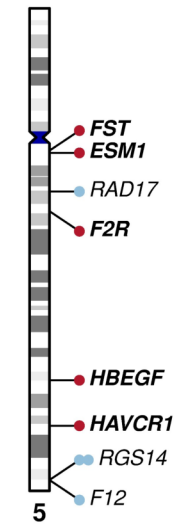
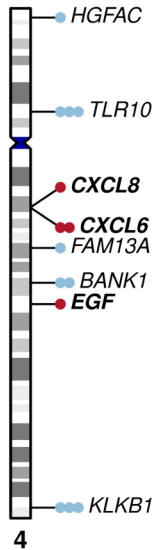
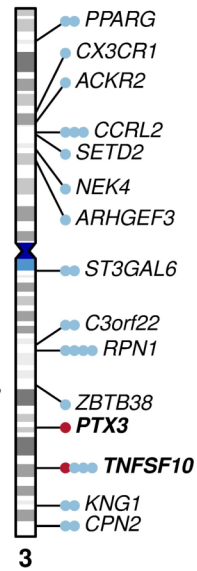
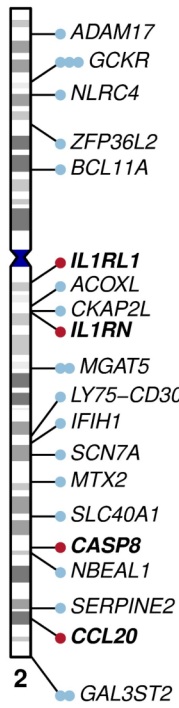
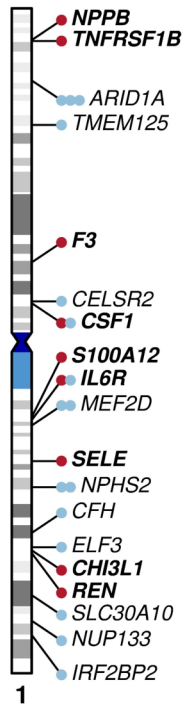
IL18: eBMD

MMP-12: eczema

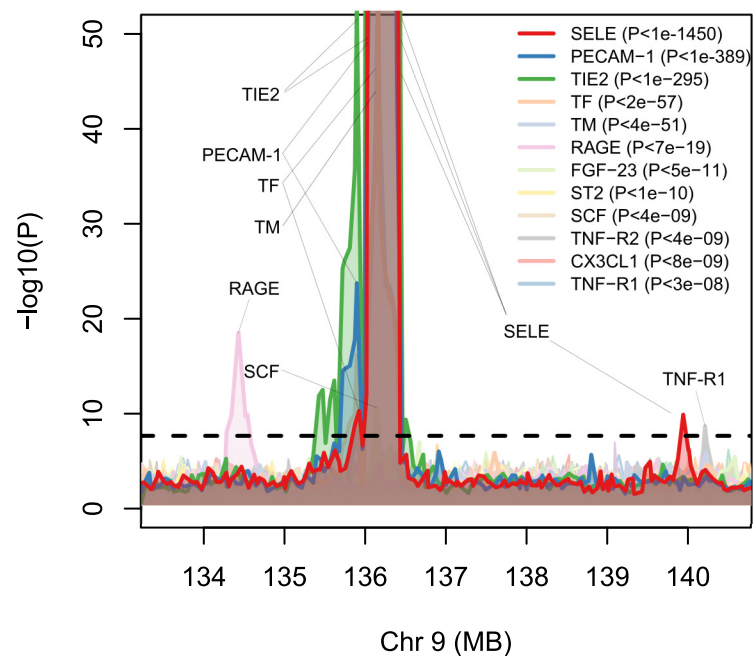
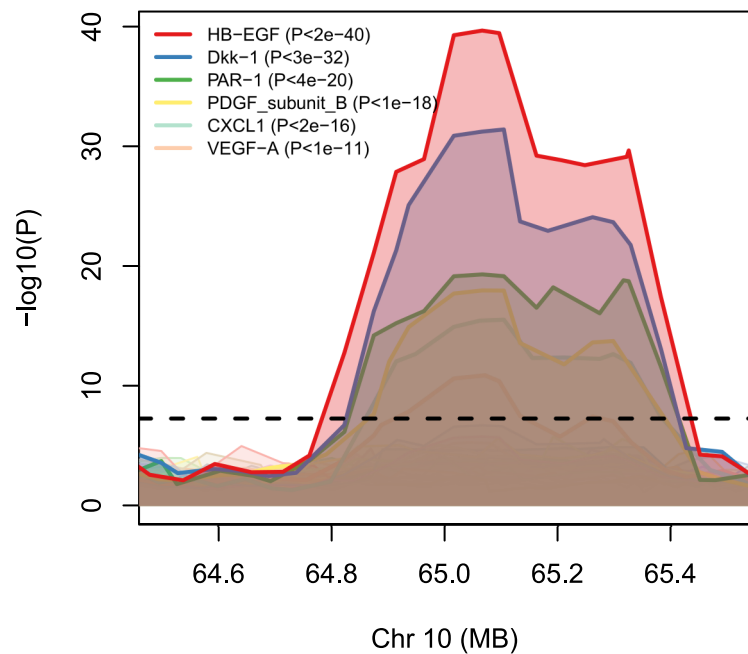
PIGF: CHD, eBMD

RAGE: Lipids, BMI, T2D,  
prostate cancer, SCZ

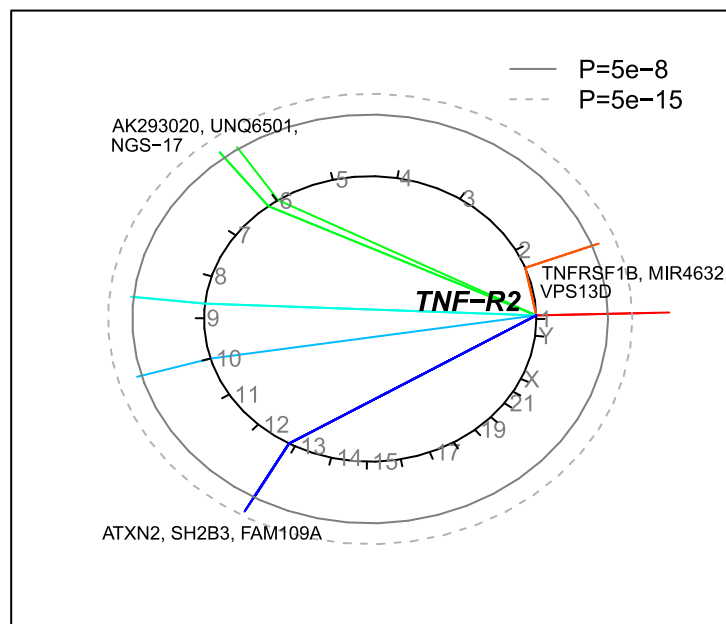
ST2: IBD\*



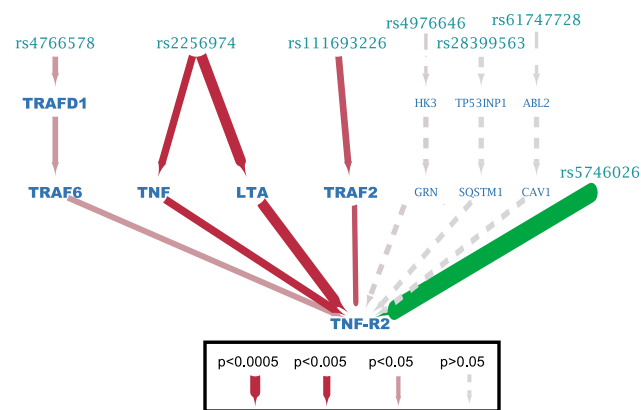
A)



B)



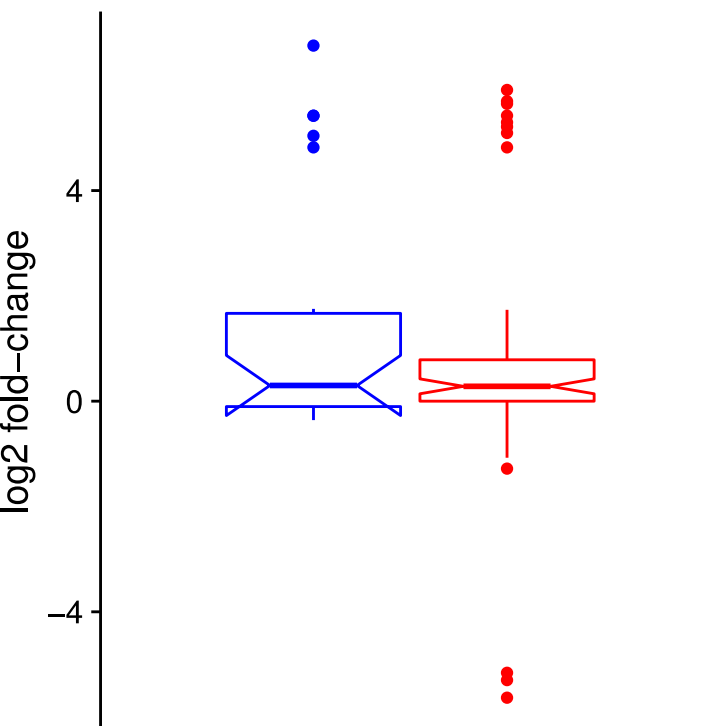
C)



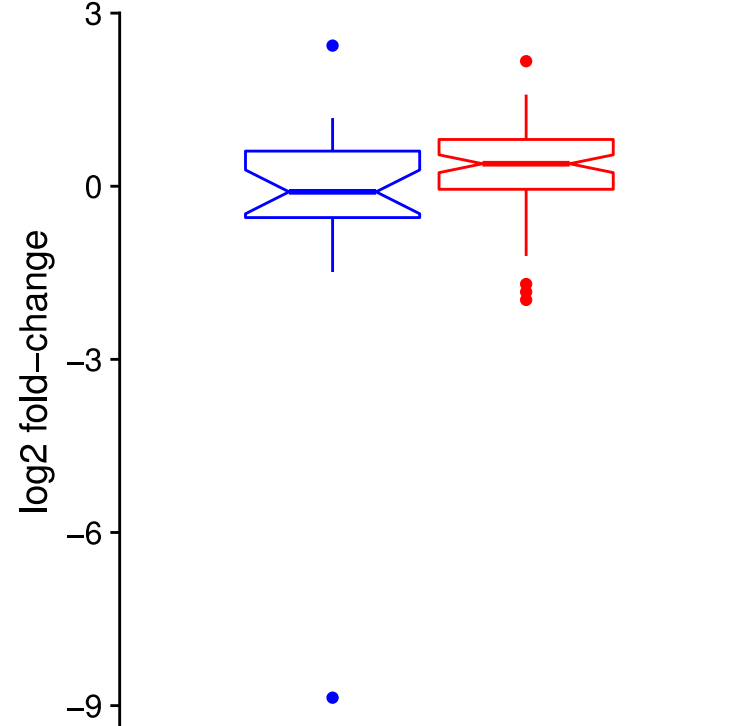


.	.	.	0.35	.	.	.	.	.	.	.	2.96e-05	0.51	.	.	.	.	.	0.5	AGER		
0.53	0.2	0.23	.	.	0.61	.	0.29	0.24	0.31	.	0.3	0.29	0.54	0.14	.	0.8	0.29	0.03	0.26	CASP8	
.	.	.	2.4e-11	.	.	.	.	.	.	0.69	4.31e-13	.	.	.	.	.	.	.	.	CCL3	
3.59e-05	.	.	0.00015	.	.	.	.	7.28e-05	.	.	2.9e-05	4.98e-05	.	.	2.65e-05	.	.	1.38e-05	5.56e-05	CCL4	
3.03e-41	7.19e-55	5.52e-44	9.93e-44	.	1.17e-33	.	4.12e-36	3.14e-46	3.61e-39	.	1.79e-51	5.39e-20	3.23e-42	.	.	.	4.29e-44	5.54e-38	5.83e-22	CD40	
1.66e-108	.	.	.	.	3.4e-113	.	6.44e-99	.	1.05e-85	9.96e-111	3.58e-18	2.47e-09	1.85e-115	.	0.53	1.4e-100	.	.	2.51e-86	CHI3L1	
0.018	.	0.0022	0.61	.	0.12	.	.	.	.	.	.	0.1	.	0.29	.	.	.	.	.	CSF1	
5.89e-39	1.03e-38	0.028	1.67e-22	4.94e-28	0.0092	1.21e-38	2.95e-19	9.28e-39	4.37e-05	.	8.22e-36	1.5e-38	1.39e-31	0.073	0.25	6.45e-38	2.35e-35	.	4.63e-37	CSTB	
.	.	.	.	.	.	.	.	.	.	.	.	1.8e-26	.	.	.	.	.	.	.	CTSD	
0.023	.	.	.	.	.	.	.	.	.	0.17	.	.	.	.	.	.	.	0.76	.	CTSL	
.	.	0.38	0.00038	.	.	.	.	.	.	.	.	.	.	.	.	.	.	5.44e-09	.	CX3CL1	
.	0.0095	.	.	.	0.02	5.44e-09	0.0093	0.0095	.	.	0.011	.	0.0085	.	.	.	.	0.55	0.017	CXCL16	
0.079	0.018	0.27	0.87	0.53	0.2	.	0.0058	0.42	0.27	0.23	0.45	0.35	0.44	0.063	.	0.91	0.69	0.94	0.43	F2R	
0.00027	1.72e-05	0.83	.	0.055	.	.	.	0.053	4.84e-06	.	3.56e-06	1.06e-06	.	.	.	.	0.019	.	1.42e-05	FAS	
0.04	.	.	.	.	.	.	.	.	.	.	.	.	.	.	.	.	.	.	.	0.66	GAL
0.62	0.36	.	.	0.00071	.	.	7.38e-62	.	.	.	.	.	.	.	.	.	0.4	.	0.021	0.012	HAVCR1
0.014	.	.	.	.	.	0.89	.	0.18	0.011	.	0.11	.	.	.	.	0.73	.	.	.	8.26e-67	IL16
.	.	.	.	.	.	.	.	.	.	.	1.34e-07	9.05e-19	6.01e-21	.	.	.	.	0.029	.	IL18	
.	.	.	.	.	.	.	.	.	.	.	4.58e-104	.	.	.	.	.	.	.	.	IL1RL1	
6.2e-24	.	.	.	.	.	.	.	.	.	.	.	.	.	.	0.21	.	.	8.48e-19	.	IL1RN	
.	.	.	.	.	5.71e-282	7.78e-05	.	1.97e-158	.	.	.	.	.	.	7.32e-56	.	.	.	9.25e-279	IL6R	
.	.	.	.	.	.	.	.	.	.	0.059	.	.	0.054	0.0043	.	.	.	.	.	KLK11	
.	0.75	.	.	1.23e-16	1.62e-19	.	1.22e-16	0.89	3.56e-25	.	1.07e-06	.	0.00058	.	.	.	0.43	.	.	MMP1	
0.97	.	.	.	.	.	.	.	.	0.82	.	0.033	.	.	.	.	.	.	.	.	0.38	S100A12
.	.	.	.	.	0.034	.	.	.	.	0.23	.	.	.	.	.	.	.	.	.	SELE	
.	.	.	.	.	.	.	0.00025	.	.	0.0038	.	.	.	.	.	.	.	.	.	0.37	TEK
.	.	.	.	.	.	.	0.024	0.29	.	.	.	.	0.0027	.	.	.	.	0.82	.	TNFRSF11B	
Adipose Subcutaneous	Adipose Visceral Omentum	Adrenal Gland	Artery Aorta	Artery Coronary	Artery Tibial	Cells EBV-transformed Lymphocytes	Cells Transformed fibroblasts	Heart Atrial Appendage	Heart Left Ventricle	Liver	Lung	Muscle Skeletal	Pancreas	Pituitary	Small Intestine Terminal Ileum	Spleen	Stomach	Thyroid	Whole Blood		

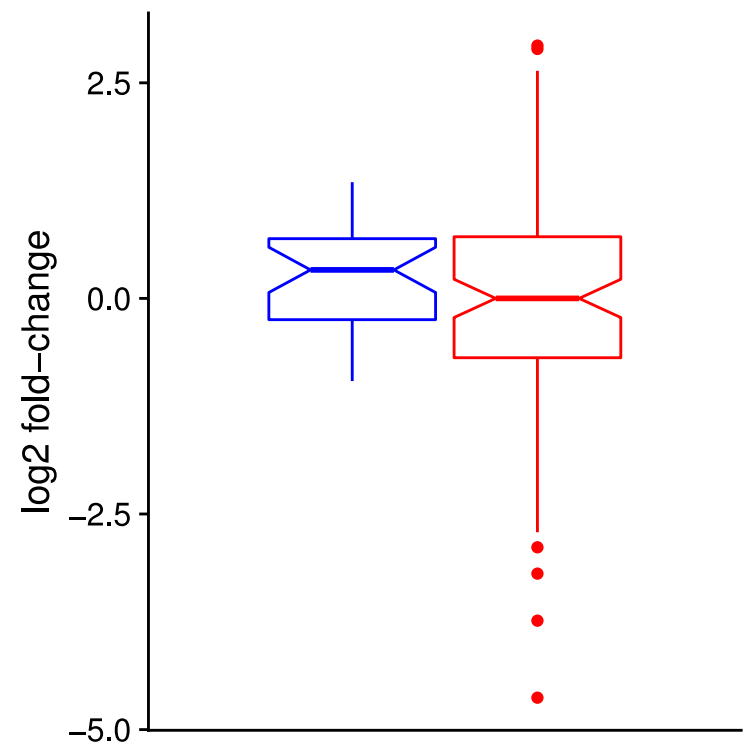


**CCL3 (MIP-1-alpha)**

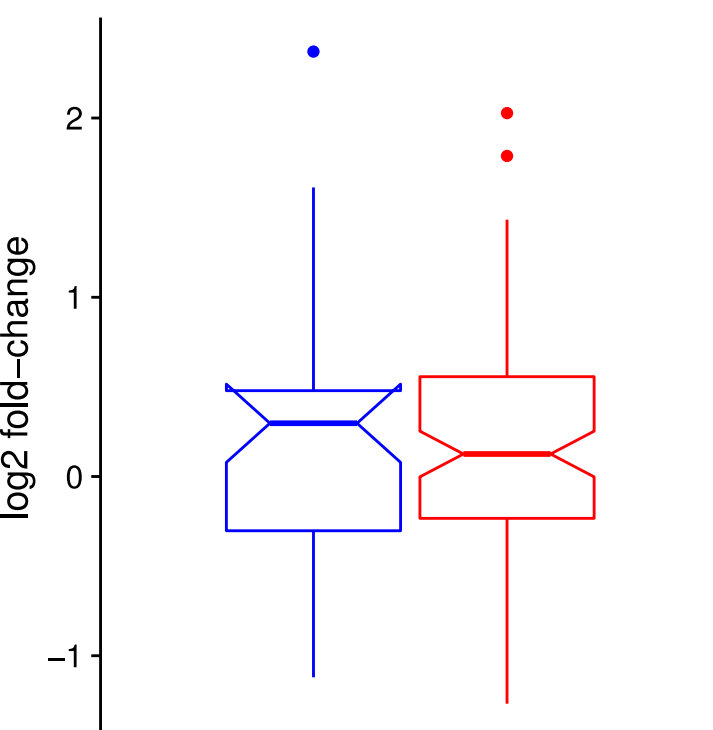
Treatment group ▢ Placebo ▢ PF-04634817

**CCL8 (MCP-2)**

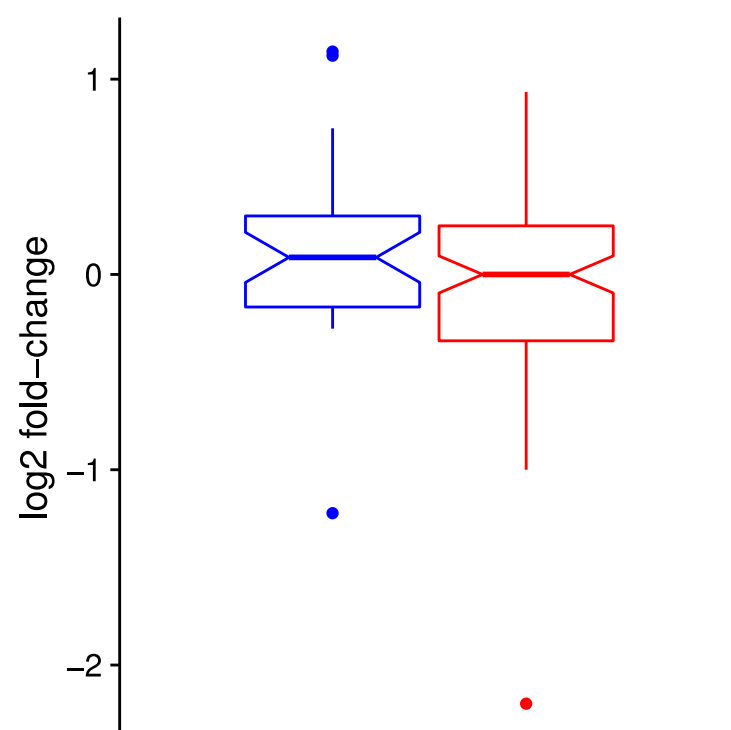
Treatment group ▢ Placebo ▢ PF-04634817

**EN-RAGE**

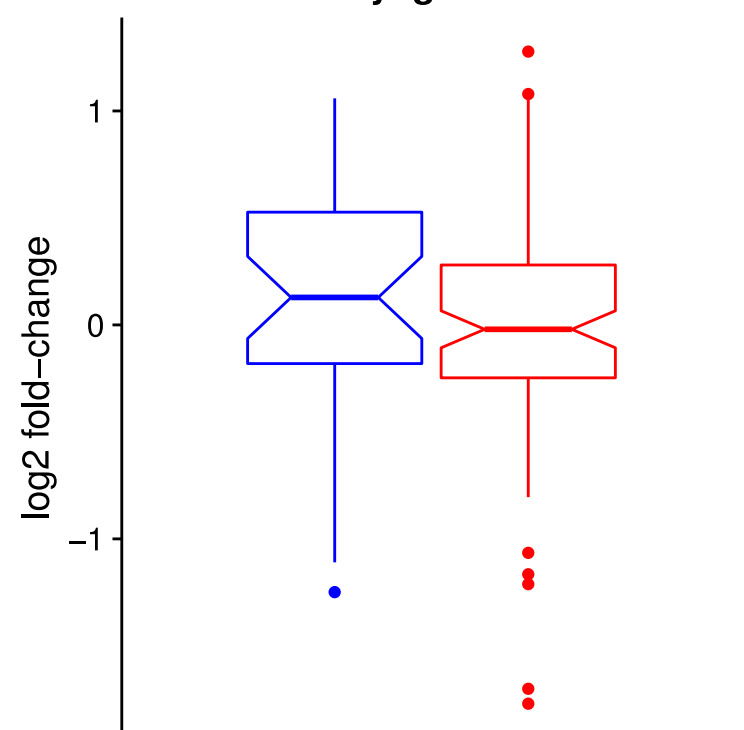
Treatment group ▢ Placebo ▢ PF-04634817

**FGF-23**

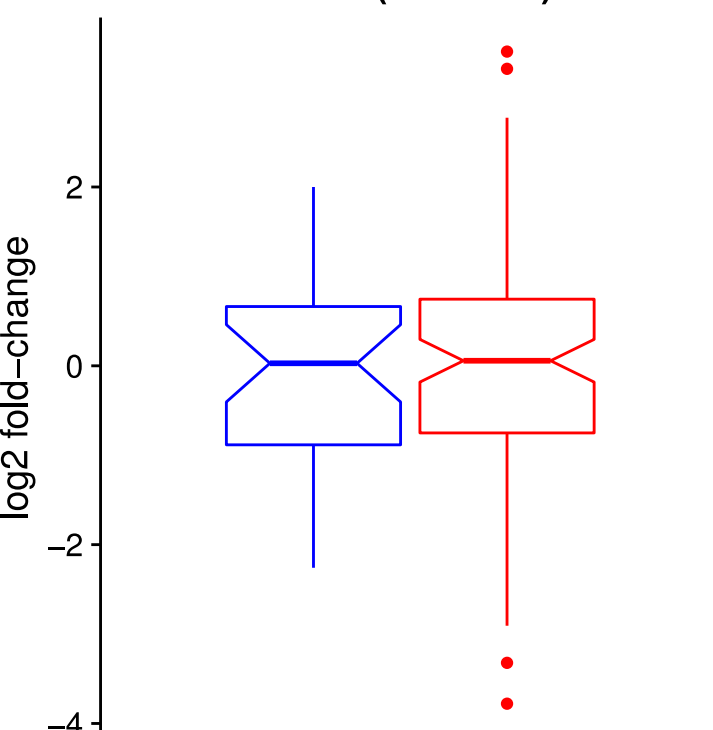
Treatment group ▢ Placebo ▢ PF-04634817

**KIM-1**

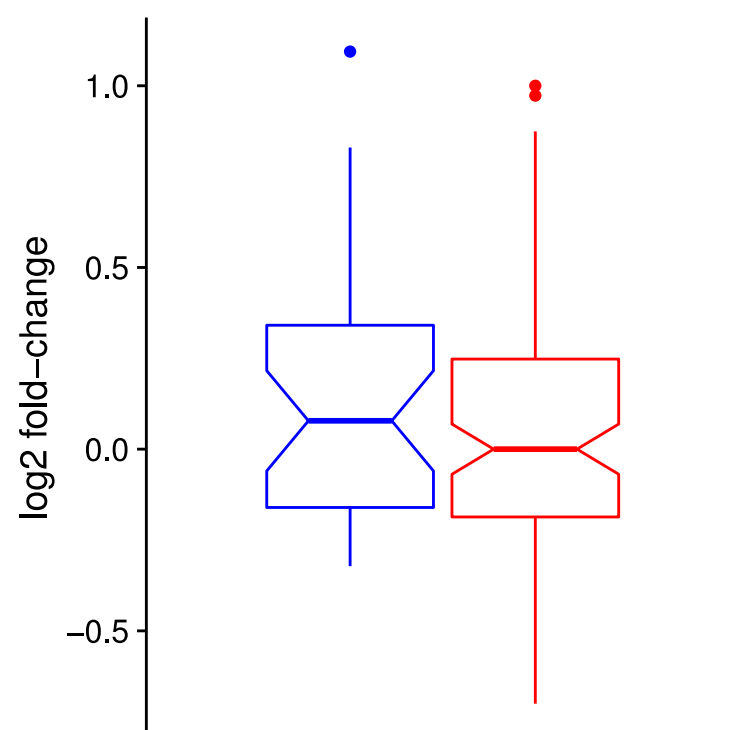
Treatment group ▢ Placebo ▢ PF-04634817

**Myoglobin**

Treatment group ▢ Placebo ▢ PF-04634817

**CCL5 (RANTES)**

Treatment group ▢ Placebo ▢ PF-04634817

**TNFR-2**

Treatment group ▢ Placebo ▢ PF-04634817

A)

## Meta analysis

Step 1:  
one file per protein per study: merge  
multi-chr, split two-study combinations,  
split one-big-file

Step 2:  
have a standardized file naming scheme,  
unify column structure and naming  
schemes, re-map the a1/a2 columns for  
indels (I/D->A/ATC)

Step 3:  
standardize markernames to  
<chr><position hg19><A1\_A2>, with  
A1\_A2 as alphabetical sort and compare  
frequencies with 1kgenomes

Step 4:  
first change in row-count: filtering SNPs  
according to imputation quality, as well  
as genotyped/imputed column ("IMP")

Step 5:  
run METAL analysis on prepared data

Sumstats data  
freeze

Sumstats data  
freeze

SNP selection criteria

"Sentinel SNP"  $P < 5e-8$   
Pruned to  $\pm 1$  MB window

Table S2  
Primary hit  
 $n_{\text{SNP}} = 401$

\*Criteria in next figure (7)

Table S2  
Instrument  
variable selected  
 $n_{\text{SNP}} = 467$

Mendelian  
Randomization

GCTA-COJO  $P < 5e-8$   
Independent signal  $< 1$  MB

Table S2  
Secondary hit  
 $n_{\text{SNP}} = 144$

P-discovery  $< 5e-8$

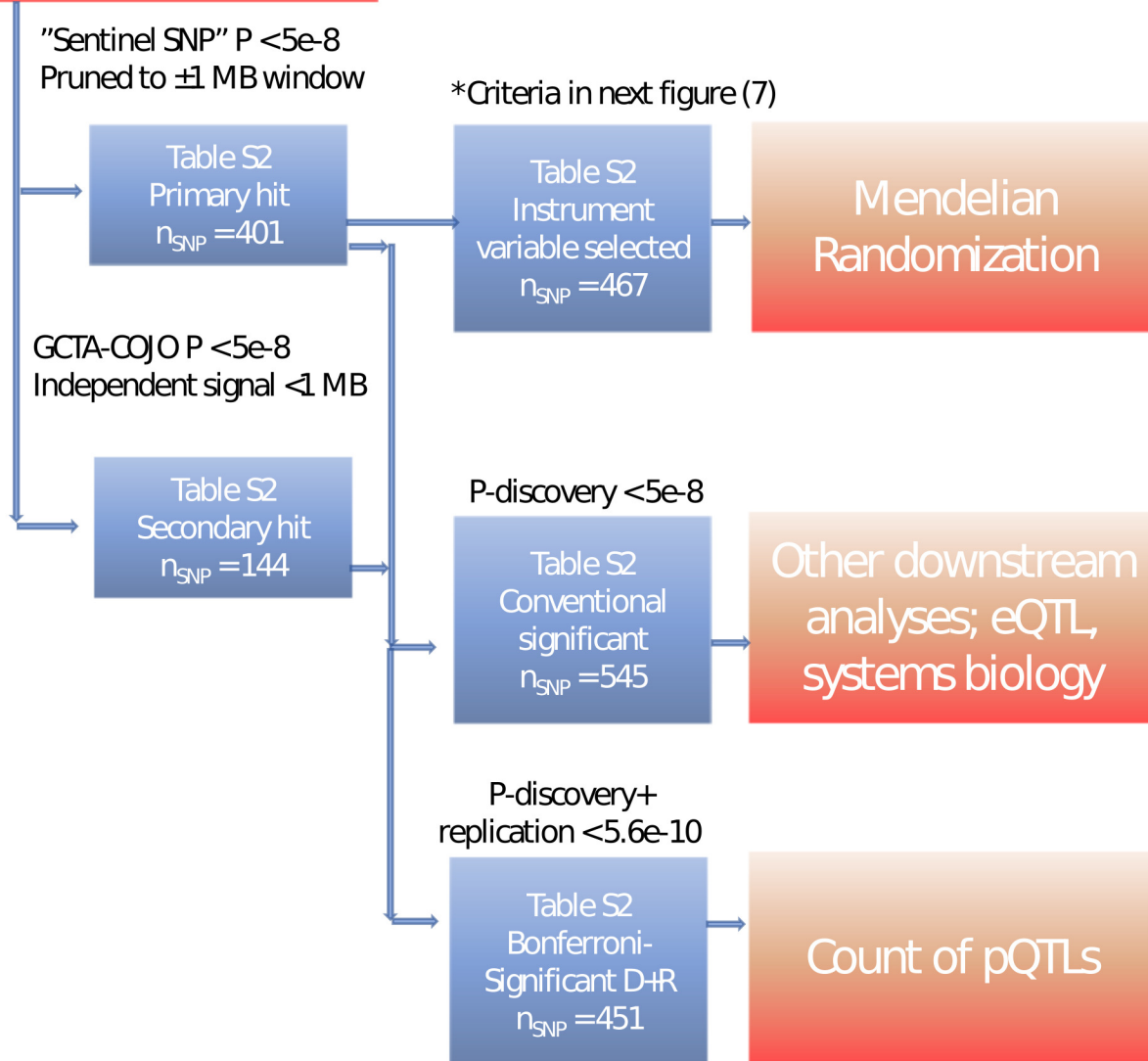
Table S2  
Conventional  
significant  
 $n_{\text{SNP}} = 545$

Other downstream  
analyses; eQTL,  
systems biology

P-discovery+  
replication  $< 5.6e-10$

Table S2  
Bonferroni-  
Significant D+R  
 $n_{\text{SNP}} = 451$

Count of pQTLs



START

